NASA

Technical Memorandum 78058

Calibration Analysis for a Multi-Channel Infrared Scanning Radiometer

Harvey Walden, Edward J. Hurley, and C. Laurence Korb

DECEMBER 1977

National Aeronautics and Space Administration

Goddard Space Flight Center
Greenbelt, Maryland 20771

TM 78058

CALIBRATION ANALYSIS FOR A MULTI-CHANNEL INFRARED SCANNING RADIOMETER

Harvey Walden
Edward J. Hurley
C. Laurence Korb

December 1977

NATIONAL AERONAUTICS AND SPACE ADMINISTRATION
GODDARD SPACE FLIGHT CENTER
Greenbelt, Maryland

CALIBRATION ANALYSIS FOR A MULTI—CHANNEL INFRARED SCANNING RADIOMETER

Harvey Walden
Edward J. Hurley
C. Laurence Korb

ABSTRACT

A procedure for calibrating an infrared scanning spectroradiometer by a computerized parametric error analysis technique is developed and described. The uncertainties in the radiometric measurements of scene radiance and (for the case of a blackbody scene) temperature due to possible uncertainties in the calibration target temperature, calibration target emissivity, and instrument temperature are calculated for a range of uncertainty levels in the parameters, as well as for a gamut of scene temperatures corresponding to a given spectral channel. This technique is applicable to the radiometric calibration of any infrared radiometer; in this paper, it has been applied specifically to the Cloud-Top Scanning (C.T.S.) Radiometer, a three-channel instrument designed for aircraft-borne cloud radiance measurements in the 6.75 and 11.5 μm thermal emission spectral regions.

CONTENTS

ILLUSTRATIONS

TABLES

INTRODUCTION

The characteristics of cloud formations, viz., water content, temperature and altitude, as well as the temperature of the land and water surface beneath the clouds, are used to predict the development of major weather patterns, in particular the occurrence and movement of severe storm centers. The determination of these characteristics by the measurement of cloud and surface thermal emission is the objective of many spacecraft- and aircraft-borne scanning spectroradiometers.

Fundamentally, a radiometer measures radiant flux within its instantaneous field of view and spectral interval. If a uniform scene fills the radiometer instantaneous field of view and radiates as a blackbody within the spectral interval, then the scene temperature can be determined from the radiance measurement, assuming the intervening path is transparent to the radiation of interest. Radiometers are generally calibrated in terms of radiance by using one or more known blackbody (or, more accurately, graybody) calibration targets. The radiometer can then measure unknown targets in terms of equivalent blackbody radiance.

The purpose of this paper is to provide and describe a procedure for calibrating a spectroradiometer by performing a computerized parametric error analysis. Errors in measured target radiance due to uncertainties in particular

instrument parameters are calculated using a range of scene temperatures for given infrared radiation spectral intervals. This procedure should be applicable to the radiometric calibration of any infrared radiometer, although initially it has been applied to the Cloud-Top Scanning (C. T. S.) Radiometer, a three-channel radiometer designed for cloud radiance measurements. The C. T. S. instrument is designed for operation on a high altitude aircraft, and it measures reflected solar radiation at 0.65 μm and thermal emission in the 6.75 and 11.5 μm spectral regions.

In the 11.5 μm atmospheric window region, clouds, water and land surface features resemble blackbodies reasonably well. Also, in this wavelength interval, reflected solar radiation is generally negligible as compared to terrestrial emission. Thus, even during daylight hours, the measured radiance temperature is close to the true target temperature. If target emissivity and atmospheric transmission are taken into account, the actual target temperature can be determined. Thus, a spectroradiometer is often utilized for its temperature discrimination capabilities.

This analysis calculates the uncertainties in radiometric measurements of scene radiance and (for the case of a blackbody scene) temperature due to uncertainties in calibration target temperature, calibration target emissivity, and instrument temperature. Errors due to such sources as signal to noise ratio and registration error are not included in this study.

ANALYSIS

The spectral projected radiance N_λ (measured in ergs/cm^3-sec-sterad, or, more commonly, in watts/cm^2-μm-sterad) of a Lambertian graybody with radiant emissivity ϵ at absolute temperature T (measured in K) is given by

$$N_\lambda(T, \epsilon) = \epsilon N_\lambda(T) , \tag{1}$$

where

$$N_\lambda(T)\, d\lambda = \frac{2hc^2 d\lambda}{\lambda^5 (e^{hc/k\lambda T} - 1)} \tag{2}$$

is the Planck radiation function for the wavelength interval λ to $\lambda + d\lambda$ (measured in cm), with the constants,

$c = 2.997925 \times 10^{10}$ cm/sec (speed of light),

$h = 6.626196 \times 10^{-27}$ erg-sec (Planck's constant),

$k = 1.380622 \times 10^{-16}$ erg/K (Boltzmann's constant).

Thus, the projected radiance N (measured in ergs/cm^2-sec-sterad, or watts/cm^2-sterad) in the wavelength interval λ_L to λ_U is

$$N(T,\epsilon) = \int_{\lambda_L}^{\lambda_U} g(\lambda) N_\lambda(T,\epsilon)\, d\lambda = \epsilon \int_{\lambda_L}^{\lambda_U} g(\lambda) N_\lambda(T)\, d\lambda , \tag{3}$$

where $g(\lambda)$ is the instrument response function. It is assumed that the emissivity ϵ is independent of wavelength and temperature for the spectral interval λ_L to λ_U. In a typical radiometer, the instrument response function is close to rectangular, and, for the sake of generality, in this work, $g(\lambda)$ is assumed to be unity in the spectral interval λ_L to λ_U and zero elsewhere.

The radiance measured by a radiometer when a calibration target fills its field of view will consist of target emission and instrument case emission

reflected by the target into the signal beam. Therefore, the calibration radiance N_{cal} is given as the sum of two terms:

$$N_{cal}(T_{cal}, T_{instr}, \epsilon) = N(T_{cal}, \epsilon) + (1 - \epsilon) N(T_{instr}, \epsilon_{instr})$$

$$= \epsilon \int_{\lambda_L}^{\lambda_U} N_\lambda(T_{cal})\, d\lambda$$

$$+ (1 - \epsilon) \int_{\lambda_L}^{\lambda_U} N_\lambda(T_{instr})\, d\lambda. \qquad (4)$$

In equation (4), ϵ is the calibration target emissivity (and, of course, $1 - \epsilon$ is the reflectivity of the calibration target), and T_{cal}, T_{instr} are the absolute temperatures of the calibration target and instrument case, respectively. It is assumed in equation (4) and for the purposes of this calculation that the emissivity ϵ_{instr} of the instrument case is unity. In the above form, it is evident that calibration of the radiometer through a parametric error analysis must consider the uncertainties in calibration target radiance N_{cal} due to uncertainties in target temperature T_{cal}, target emissivity ϵ, and instrument temperature T_{instr}. The radiation spectral interval (λ_L, λ_U) must, of course, also be specified.

Although the Planck function (2) cannot be analytically integrated by closed methods, numerical integration techniques may be applied to solve equation (4) iteratively. For instance, if the composite Simpson's rule [Ref. 1, pp. 78-79] is used, then functional values are required at $2n + 1$ spectral points, $\lambda_i = \lambda_L + iH$, $i = 0, 1, \ldots, 2n$, where H is the subinterval length, given as $H = (\lambda_U - \lambda_L)/2n$. Then n repeated applications of Simpson's rule lead to the approximation:

$$\int_{\lambda_L}^{\lambda_U} N_\lambda(T)\,d\lambda \cong \frac{H}{3}\left[N_{\lambda_0} + 4N_{\lambda_1} + 2N_{\lambda_2} + 4N_{\lambda_3} + 2N_{\lambda_4}\right.$$

$$\left. + \quad + 2N_{\lambda_{2n-2}} + 4N_{\lambda_{2n-1}} + N_{\lambda_{2n}}\right], \tag{5}$$

where

$$N_{\lambda_i} = N_{\lambda_i}(T) = \frac{2hc^2}{\lambda_i^5\left(e^{hc/k\lambda_i T} - 1\right)}, \quad i = 0, 1, \quad . \quad , 2n. \tag{6}$$

It is assumed in this study that the radiometer contains two graybody calibration targets, at known distinct temperatures, T_C and T_H, and with equal emissivities $\epsilon < 1$. In order to reduce systematic calibration errors, the known "cold" (T_C) and "hot" (T_H) calibration target temperatures should be separated as much as possible within the range of anticipated scene temperatures. It is further assumed that the radiometer detector output voltage is directly proportional to the collected radiance. Thus, it is possible to obtain a linear radiometric calibration curve using the two calibration targets at known temperatures.

To establish a nominal calibration curve, the dynamic ranges of the voltage scale and the scene radiances must be known or estimated. It is assumed here that the voltage output is 2 V_{max} full range for a given radiation spectral interval (λ_L, λ_U), and that this range has a center point of zero. Thus, the voltage output V satisfies $-V_{max} \leq V \leq V_{max}$. Furthermore, the radiometric range is specified by upper and lower limits on the anticipated scene temperatures: T_{max} and T_{min}, respectively. To convert temperature dynamic range to limits on the anticipated projected radiance, equation (3) is invoked, with ϵ assumed equal to unity:

$$N_{min} = \int_{\lambda_L}^{\lambda_U} N_\lambda (T_{min})\, d\lambda , \tag{7a}$$

$$N_{max} = \int_{\lambda_L}^{\lambda_U} N_\lambda (T_{max})\, d\lambda . \tag{7b}$$

Given the two fixed points, $(-V_{max}, N_{min})$ and (V_{max}, N_{max}), the voltage scale can be calibrated linearly with respect to projected radiance, so that

$$\frac{V + V_{max}}{N - N_{min}} = \frac{2 V_{max}}{N_{max} - N_{min}} ,$$

or

$$V = \left(\frac{2 V_{max}}{N_{max} - N_{min}} \right) (N - N_{min}) - V_{max} , \tag{8}$$

where V is a voltage in the range $|V| \leq V_{max}$ corresponding to an arbitrary radiance measurement N such that $N_{min} \leq N \leq N_{max}$. If the radiance measurement falls outside this range, then the linear calibration relation (8) still applies, but the corresponding voltage may be off-scale, i.e., $|V| > V_{max}$.

For the two calibration targets with temperatures T_C and T_H and emissivity ϵ, corresponding nominal projected "cold" and "hot" radiances are, respectively,

$$N_C = \epsilon \int_{\lambda_L}^{\lambda_U} N_\lambda (T_C)\, d\lambda + (1 - \epsilon) \int_{\lambda_L}^{\lambda_U} N_\lambda (T_{instr})\, d\lambda , \tag{9a}$$

$$N_H = \epsilon \int_{\lambda_L}^{\lambda_U} N_\lambda(T_H)\, d\lambda + (1-\epsilon) \int_{\lambda_L}^{\lambda_U} N_\lambda(T_{instr})\, d\lambda , \qquad (9b)$$

by equation (4). The corresponding "cold" and "hot" voltages are found by substitution into equation (8), as follows:

$$V_C = \left(\frac{2\,V_{max}}{N_{max} - N_{min}}\right)(N_C - N_{min}) - V_{max} , \qquad (10a)$$

$$V_H = \left(\frac{2\,V_{max}}{N_{max} - N_{min}}\right)(N_H - N_{min}) - V_{max} . \qquad (10b)$$

Subtraction of equation (10a) from equation (10b) yields

$$\frac{V_H - V_C}{N_H - N_C} = \frac{2\,V_{max}}{N_{max} - N_{min}} ,$$

so that, using the two fixed points, (N_C, V_C) and (N_H, V_H), the nominal linear calibration relation may be written

$$V = \left(\frac{V_H - V_C}{N_H - N_C}\right)(N - N_C) + V_C . \qquad (11)$$

This is equivalent to equation (8).

Each of the three parameters consisting of the graybody calibration target temperatures, the calibration target emissivities, and the instrument temperature was varied separately in order to isolate the effects of uncertainties in each parameter on the calibration accuracy. The uncertainties in the "cold" and "hot" calibration target temperatures and emissivities were assumed to be equal, in this study. If slight changes are introduced in the values of any one of the three parameters, then the nominal calibration curve is shifted somewhat. Assume that N_C^- and N_C^+ are projected "cold" radiances, ordered such that $N_C^- < N_C < N_C^+$, corresponding to equal in magnitude but opposite in sign changes about the nominal value in any one of the three parameters, T_C, ϵ, or T_{instr}, where the other two parameters are maintained at the nominal values. Analogously, let N_H^- and N_H^+ represent projected "hot" radiances, ordered such that $N_H^- < N_H < N_H^+$, corresponding to like changes about the nominal value in any one of T_H, ϵ, or T_{instr}, with the remaining two parameters at nominal values. For example, for parametric changes ΔT in the graybody calibration target temperatures, $N_C^- = N_{cal}\ (T_C - \Delta T, T_{instr}, \epsilon)$, $N_C^+ = N_{cal}\ (T_C + \Delta T, T_{instr}, \epsilon)$, $N_H^- = N_{cal}\ (T_H - \Delta T, T_{instr}, \epsilon)$, and $N_H^+ = N_{cal}\ (T_H + \Delta T, T_{instr}, \epsilon)$, using the functional notation of equation (4).

The projected radiances, N_C^-, N_C^+, N_H^-, and N_H^+, are used in this study to construct upper and lower calibration envelopes, as illustrated in Figure 1. The envelopes bound all possible non-nominal calibration curves which are determined by any two points, (N_1, V_C) and (N_2, V_H), such that $N_C^- \leq N_1 \leq N_C^+$ and $N_H^- \leq N_2 \leq N_H^+$.

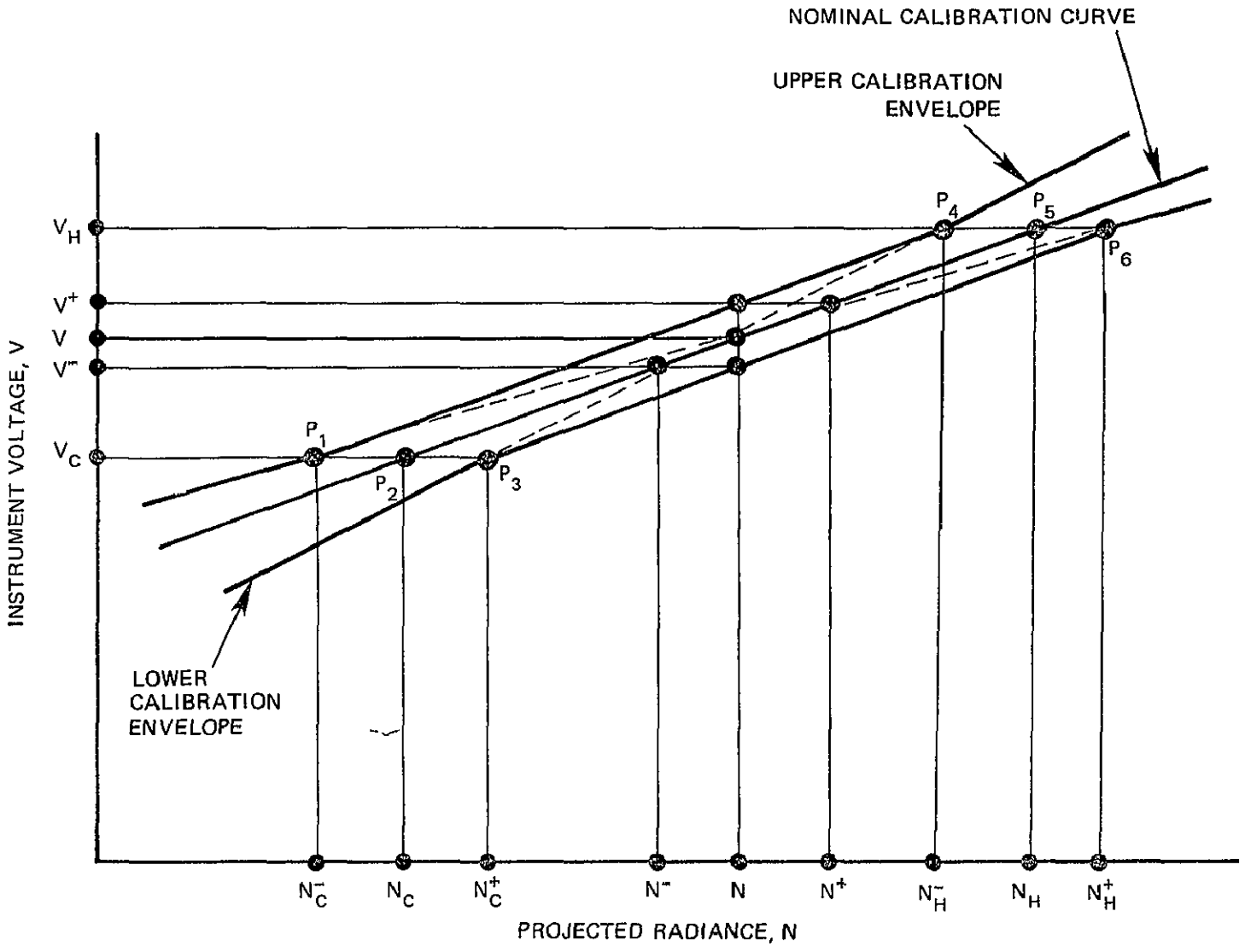

Figure 1. The nominal calibration curve and the upper and lower calibration envelopes are determined by six fixed points

The upper and lower calibration envelopes are each formed by three joined linear segments, such that the central segments are parallel (or nearly so) to the nominal calibration curve, while the outer segments diverge. Specifically, with reference to Figure 1, the upper calibration envelope is formed of the linear segments defined by P_1 and P_6 (for $V \leq V_C$ and $N \leq N_C^-$), by P_1 and P_4 (for $V_C \leq V \leq V_H$ and $N_C^- \leq N \leq N_H^-$), and by P_3 and P_4 (for $V \geq V_H$ and $N \geq N_H^-$). The lower calibration envelope is formed of the linear segments defined by P_3 and P_4 (for $V \leq V_C$ and $N \leq N_C^+$), by P_3 and P_6 (for $V_C \leq V \leq V_H$ and $N_C^+ \leq N \leq N_H^+$), and by P_1 and P_6 (for $V \geq V_H$ and $N \geq N_H^+$). The voltage and radiance values contained within the envelopes correspond to all possible values within the accuracy of the calibration, and hence extreme values on the envelopes correspond to the uncertainties in radiometric calibration resulting from the uncertainties in a given parameter, viz., T_{cal}, ϵ, or T_{instr}. In this study, a distinct pair of calibration envelopes was constructed for each variation (i.e., assumed uncertainty) of the single parameters, T_{cal}, ϵ, and T_{instr}.

For a given pair of calibration envelopes, the uncertainties in the observed scene radiance and in the observed scene temperature may be determined for a range of scene temperatures T, such that $T_{min} \leq T \leq T_{max}$. For each scene temperature T, a corresponding scene projected radiance N is calculated by equation (3), assuming the scene consists of a blackbody target ($\epsilon = 1$). The radiance N is converted to a corresponding voltage V through the nominal calibration curve (11). Furthermore, the upper and lower calibration envelopes

determine a corresponding "high voltage" V^+ and "low voltage" V^-, respectively, given by

$$V^+ = \begin{cases} \left(\frac{V_H - V_C}{N_H^+ - N_C^-}\right)(N - N_C^-) + V_C, & \text{if } N \le N_C^-, \\ \left(\frac{V_H - V_C}{N_H^- - N_C^-}\right)(N - N_C^-) + V_C, & \text{if } N_C^- \le N \le N_H^-, \\ \left(\frac{V_H - V_C}{N_H^- - N_C^+}\right)(N - N_C^+) + V_C, & \text{if } N \ge N_H^-, \end{cases} \tag{12a}$$

and

$$V^- = \begin{cases} \left(\frac{V_H - V_C}{N_H^- - N_C^+}\right)(N - N_C^+) + V_C, & \text{if } N \le N_C^+, \\ \left(\frac{V_H - V_C}{N_H^+ - N_C^+}\right)(N - N_C^+) + V_C, & \text{if } N_C^+ \le N \le N_H^+, \\ \left(\frac{V_H - V_C}{N_H^+ - N_C^-}\right)(N - N_C^-) + V_C, & \text{if } N \ge N_H^+. \end{cases} \tag{12b}$$

The above high and low voltages are then converted back to corresponding high and low projected radiances, N^+ and N^-, respectively, through use of the nominal calibration curve (11), as follows:

$$N^+ = \left(\frac{N_H - N_C}{V_H - V_C}\right)(V^+ - V_C) + N_C, \tag{13a}$$

$$N^- = \left(\frac{N_H - N_C}{V_H - V_C}\right)(V^- - V_C) + N_C. \tag{13b}$$

The high and low projected radiances are the uncertainties in the scene projected radiance N due to uncertainties in any one of the three parameters, T_{cal}, ϵ, or T_{instr}, represented by the calibration envelopes about the nominal calibration curve (refer to Figure 1). Relative changes in the nominal projected radiance N are given by

$$\frac{\Delta N^+}{N} = \frac{N^+ - N}{N}, \tag{14a}$$

$$\frac{\Delta N^-}{N} = \frac{N^- - N}{N}. \tag{14b}$$

The conversion of N^+ and N^- to corresponding blackbody temperatures involves inverting the integrals,

$$N^+ = \int_{\lambda_L}^{\lambda_U} N_\lambda(T^+)\, d\lambda, \tag{15a}$$

$$N^- = \int_{\lambda_L}^{\lambda_U} N_\lambda(T^-)\, d\lambda, \tag{15b}$$

and solving for the high and low temperatures, T^+ and T^-, respectively. Since the integral equations (15) are intractable with respect to analytical inversion by closed methods, an iterative computational procedure has been applied. One such method, which has the advantage of not requiring the evaluation of derivatives, is the method of false position [Ref. 1, p. 178; Ref. 2, pp. 13ff]. If T_i^+ is the i-th approximation to the desired temperature T^+, then the following recurrence relation provides an improved approximation:

$$T^{+}_{i+1} = \frac{T(N^{+}_{i} - N^{+}) - T^{+}_{i}(N - N^{+})}{N^{+}_{i} - N}, \quad i = 1,2,3, \ . \ , \tag{16}$$

where T is the known scene temperature, N is the corresponding scene projected radiance calculated by equation (3), and $N^{+}_{i} = N(T^{+}_{i}, \epsilon = 1)$, using the functional notation of equation (3). Similarly, if T^{-}_{i} is the i-th approximation to the desired temperature T^{-}, then the method of false position provides the following recurrence relation for the improved approximation:

$$T^{-}_{i+1} = \frac{T(N^{-}_{i} - N^{-}) - T^{-}_{i}(N - N^{-})}{N^{-}_{i} - N}, \quad i = 1,2,3, \ . \ , \tag{17}$$

where $N^{-}_{i} = N(T^{-}_{i}, \epsilon = 1)$, in the notation of equation (3). Convergence for these iterative procedures occurs when, for a sufficient number of iterations,

$$\left| T^{+}_{i+1} - T^{+}_{i} \right| < \epsilon^{+} \tag{18a}$$

and

$$\left| T^{-}_{i+1} - T^{-}_{i} \right| < \epsilon^{-}, \tag{18b}$$

where $0 < \epsilon^{+}, \epsilon^{-} << 1$ are suitable pre-selected convergence criteria. The absolute changes in the nominal scene temperature T, corresponding to the observed scene radiance N, are, of course, $\Delta T^{+} = T^{+} - T$ and $\Delta T^{-} = T^{-} - T$.

NUMERICAL RESULTS

The methods previously described for calibration of a radiometer through a parametric error analysis have been applied to the Cloud-Top Scanning (C.T.S.) Radiometer. Significant parameters for the infrared channels of the C.T.S. radiometer [Ref. 3], as pertain to the current study, are displayed in Table 1.

Calculated values for parameters derived from those in Table 1, through equations (7), (9), and (10), are included in Table 2, for each of the two infrared spectral channels. Using the parameter values in Table 2, graphs of the nominal linear calibration curves (11) of voltage output vs. projected radiance were constructed for the two infrared channels and are shown in Figure 2. A voltage of -5 v corresponds to the minimum scene projected radiance N_{min} at scene temperature T_{min}, and, similarly, +5 v corresponds to the maximum scene projected radiance N_{max} at temperature T_{max}. The points labeled "240 K" and "280 K" indicate the cold and hot graybody target projected radiances, N_C and N_H, at corresponding voltage outputs, V_C and V_H, respectively.

Calibration envelopes were constructed, as described previously, for the following variations, or assumed uncertainties, in the nominal values of the graybody calibration target temperatures and emissivities and of the instrument temperature:

$$\Delta T = \Delta T_C = \Delta T_H = \pm 0.1, \pm 0.2, \pm 0.5, \pm 1.0 \text{ K}$$

$$\Delta \epsilon = \pm 0.001, \pm 0.005, \pm 0.01, \pm 0.02 \qquad (19)$$

$$\Delta T_{instr} = \pm 1, \pm 2, \pm 5, \pm 10 \text{ K}$$

Corresponding uncertainties in the observed scene radiances and temperatures were calculated for each pair of calibration envelopes for scene temperatures T

Table 1

Nominal Values of Instrument Parameters

Parameter Description and Symbol	Numerical Value and Units
Infrared spectral interval, λ_L to λ_U	Channel 2: 6.6 to 6.9 x 10^{-4} cm | Channel 3: 10.5 to 12.5 x 10^{-4} cm
Graybody calibration target temperatures, T_C, T_H	240 K, 280 K
Instrument case temperature, T_{instr}	255 K
Graybody calibration target radiant emissivity, ϵ	0.98
Full scale instrument voltage output, V_{max}	5.0 volts
Scene temperature range, T_{min} to T_{max}	Channel 2: 165 to 285 K | Channel 3: 165 to 325 K

Table 2

Calculated Values of Derived Parameters

Parameter Description and Symbol		Numerical Value and Units*	
		Channel 2	Channel 3
Scene projected radiance range	N_{min}	6.273	600.727
	N_{max}	1440.208	25710.952
Graybody target projected radiances	N_C	359.198	6486.983
	N_H	1246.846	13576.044
Graybody target voltage outputs	V_C	-2.539	-2.656
	V_H	3.652	0.167

*All projected radiances are in units of ergs/cm^2-sec-sterad and all voltages are in volts.

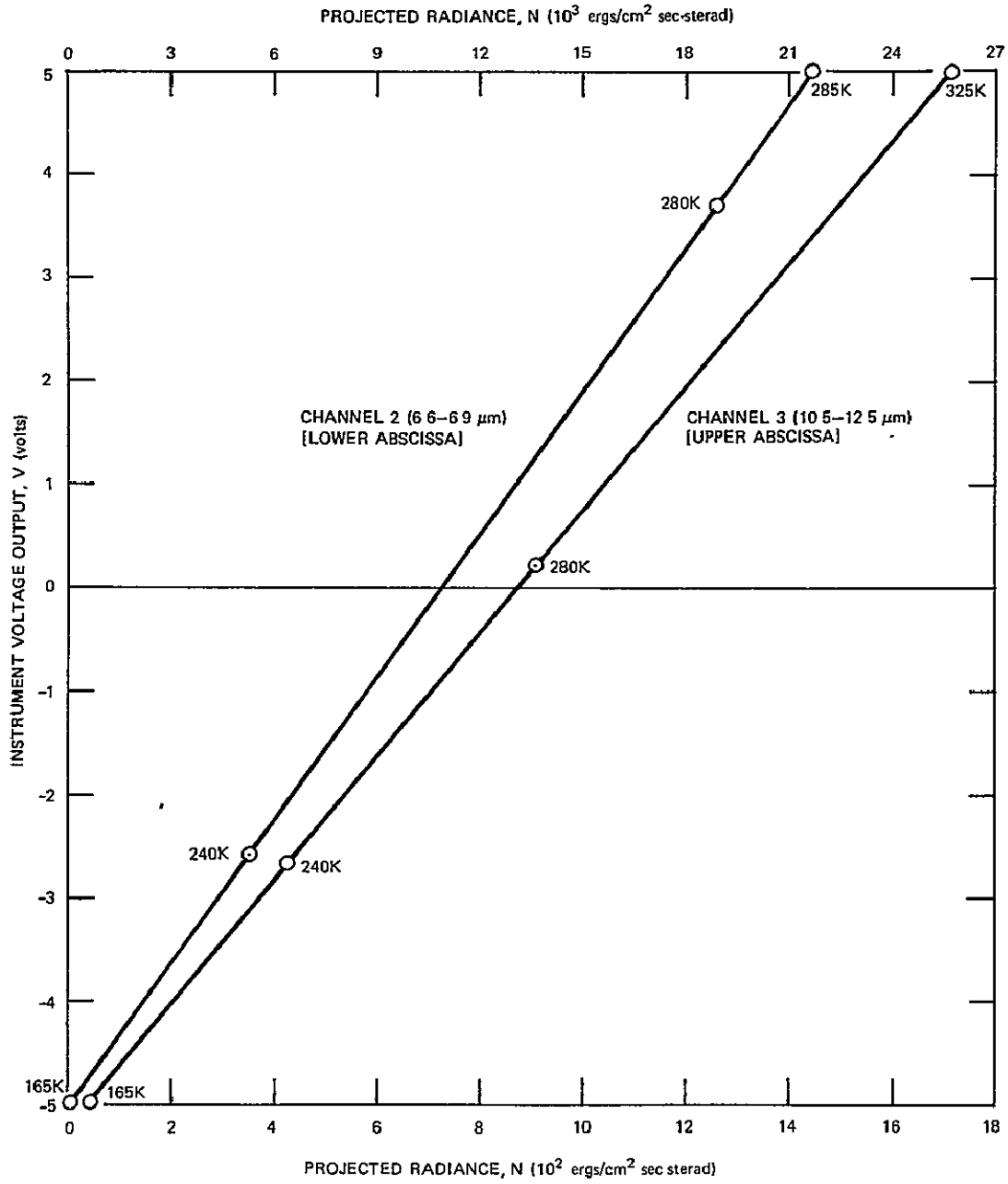

Figure 2. The nominal linear calibration curves of instrument voltage output vs. projected radiance for the two infrared spectral channels

in the range $T_{min} \leq T \leq T_{max}$ at intervals of 20 K for each of the two infrared spectral channels. The results for all 12 pairs of calibration envelopes (four variations for each of three parameters, as listed above) for each of the two spectral channels are included in Tables A1 through A24 in Appendix A. Each of these tables includes the high and low scene projected radiances, N^+ and N^-, and the high and low scene temperatures, T^+ and T^-, as well as the respective relative and absolute changes from nominal values in each scene radiance N and temperature T. Appendix B contains numerical details on the iterative procedures used in integrating the Planck function and inverting the scene radiance integrals (15) to solve for the scene temperatures.

The results included in the tables in Appendix A are summarized in Figures 3 through 8, in which the absolute changes ΔT^+, ΔT^- in scene temperature are shown as a function of scene temperature T for a given set of variations in the nominal values of the instrument parameters. These scene temperature uncertainty curves will be discussed in the following section.

In order to assess the effects of a change in the nominal values of the instrument parameters, as given in Table 1, a supplementary set of results was generated in which the nominal graybody calibration target radiant emissivity ϵ was assumed to be either 0.96 or 0.99, as contrasted with the nominal value of 0.98 assumed previously. Calibration envelopes were constructed for the set of variations in the nominal instrument temperature parameter ΔT_{instr} only, as given in the final line of (19). The results are displayed in Figures 9 through 12 as

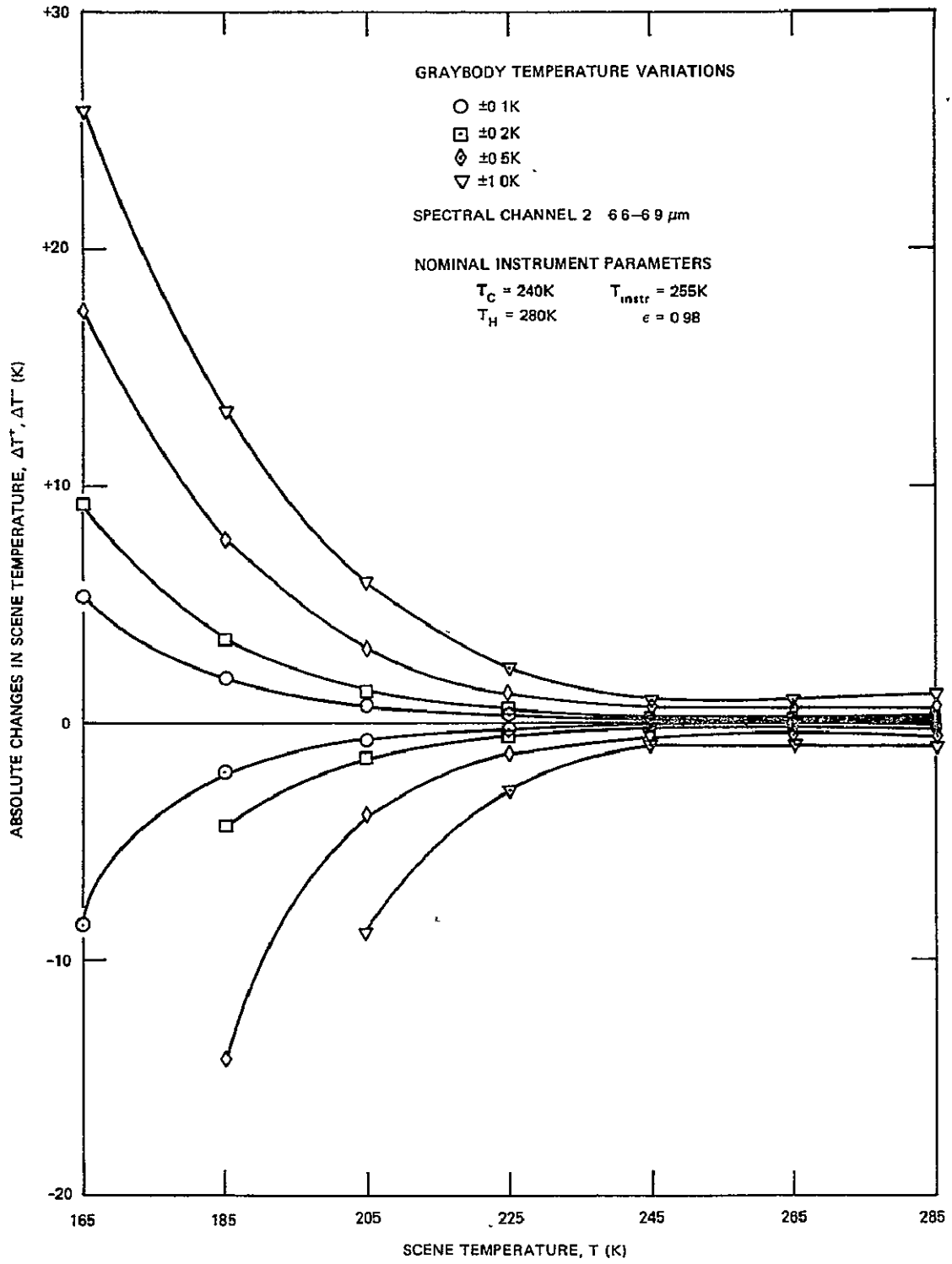

Figure 3. Scene temperature uncertainty curves due to graybody calibration target temperature variations about nominal (spectral channel 2)

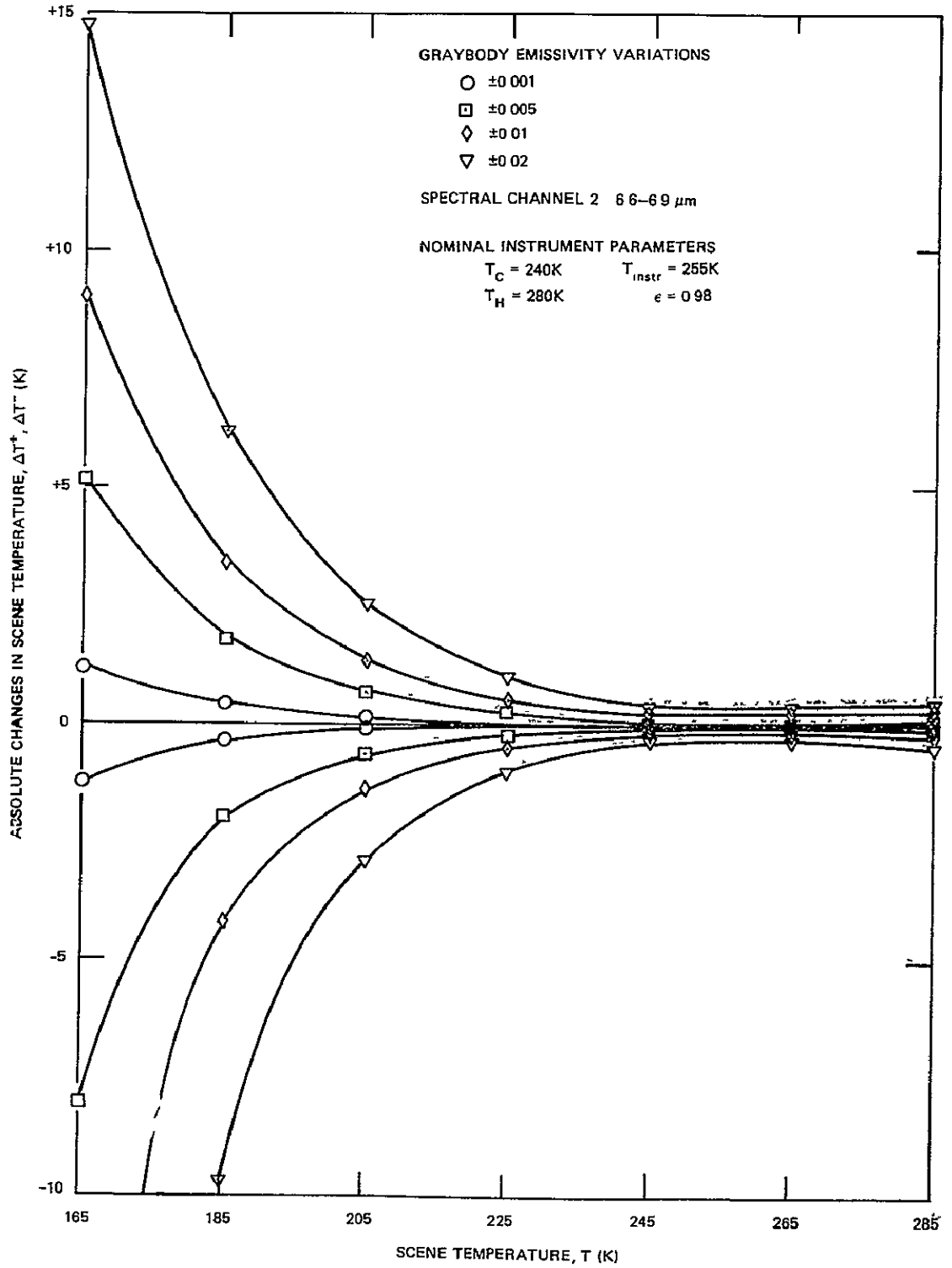

Figure 4. Scene temperature uncertainty curves due to graybody calibration target emissivity variations about nominal (spectral channel 2)

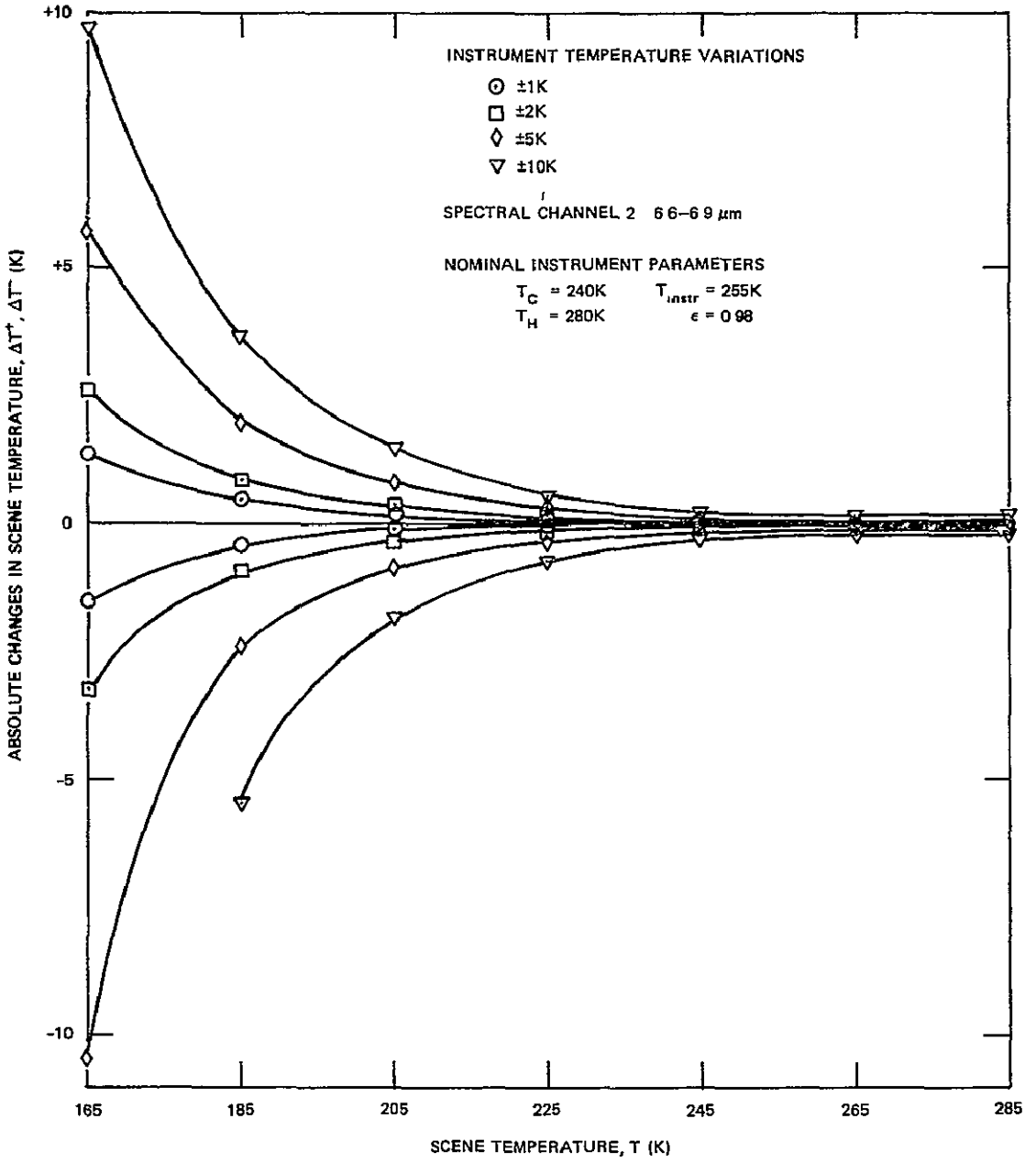

Figure 5. Scene temperature uncertainty curves due to instrument temperature variations about nominal (spectral channel 2)

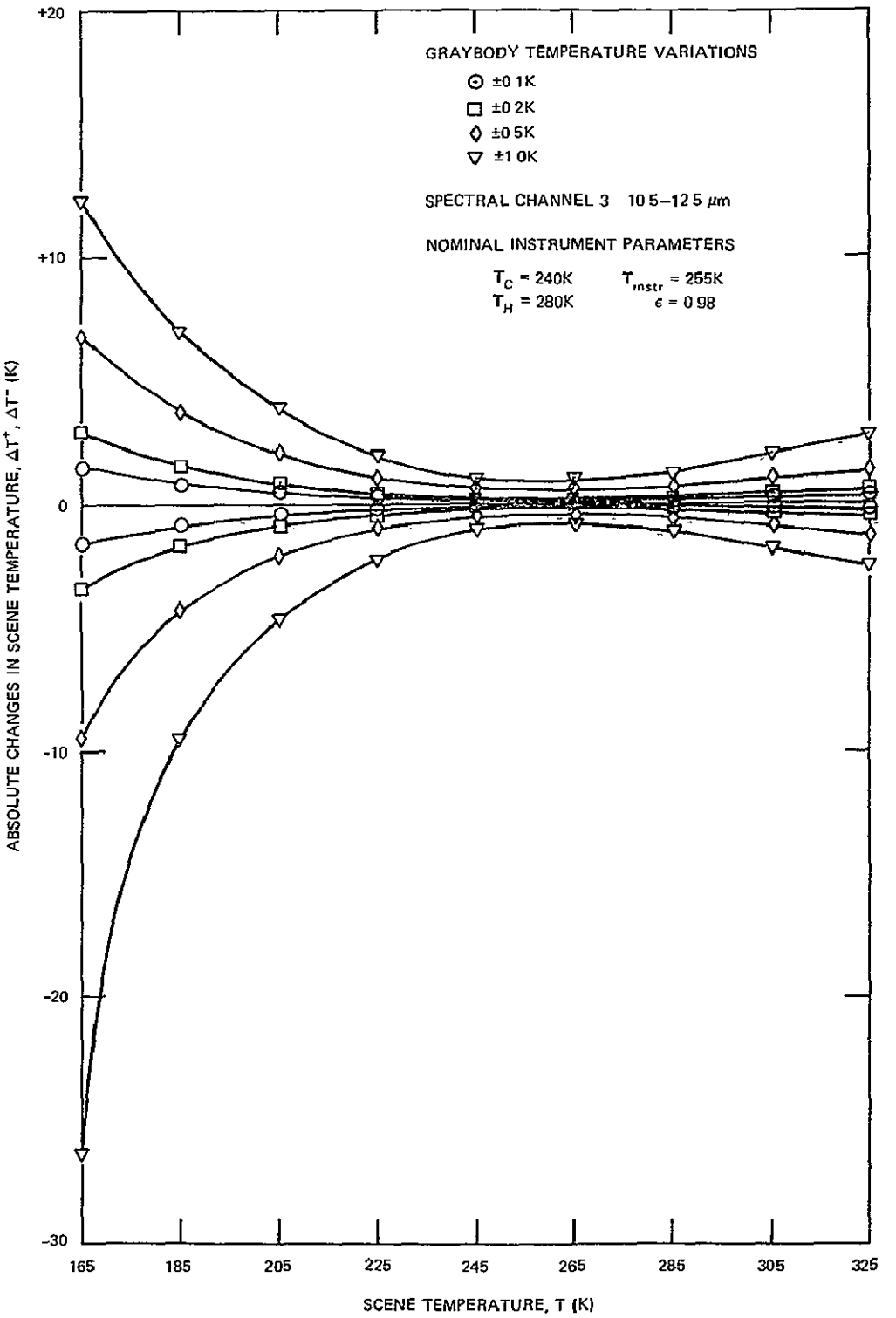

Figure 6. Scene temperature uncertainty curves due to graybody calibration target temperature variations about nominal (spectral channel 3)

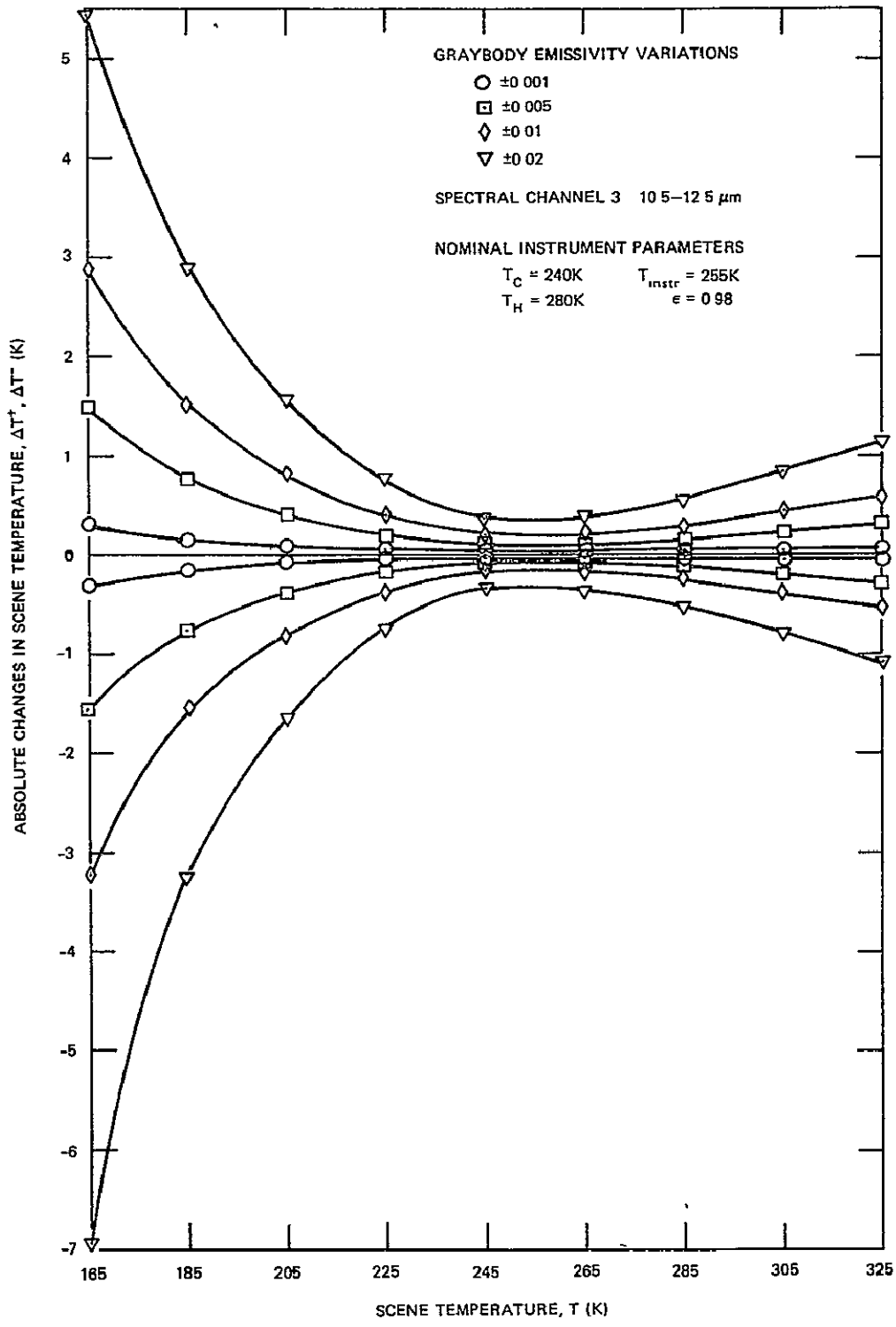

Figure 7. Scene temperature uncertainty curves due to graybody calibration target emissivity variations about nominal (spectral channel 3)

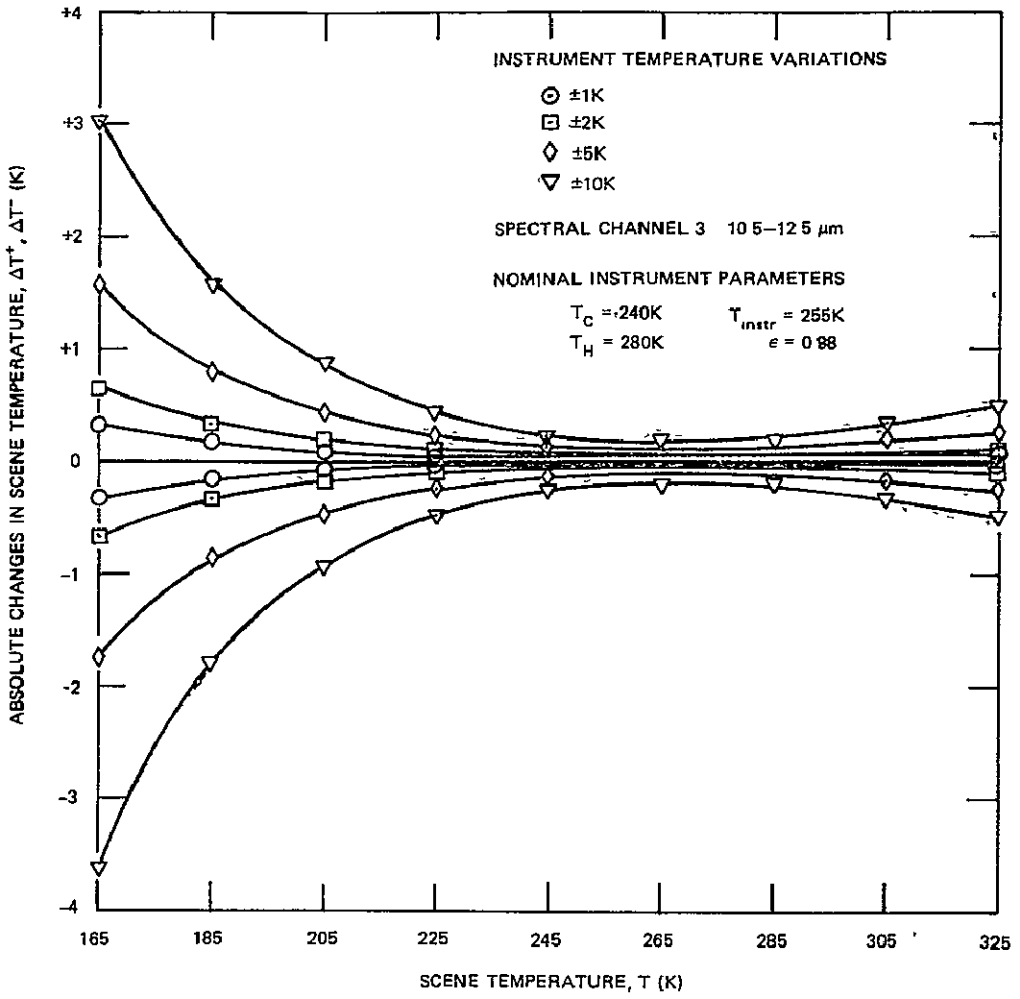

Figure 8. Scene temperature uncertainty curves due to instrument temperature variations about nominal (spectral channel 3)

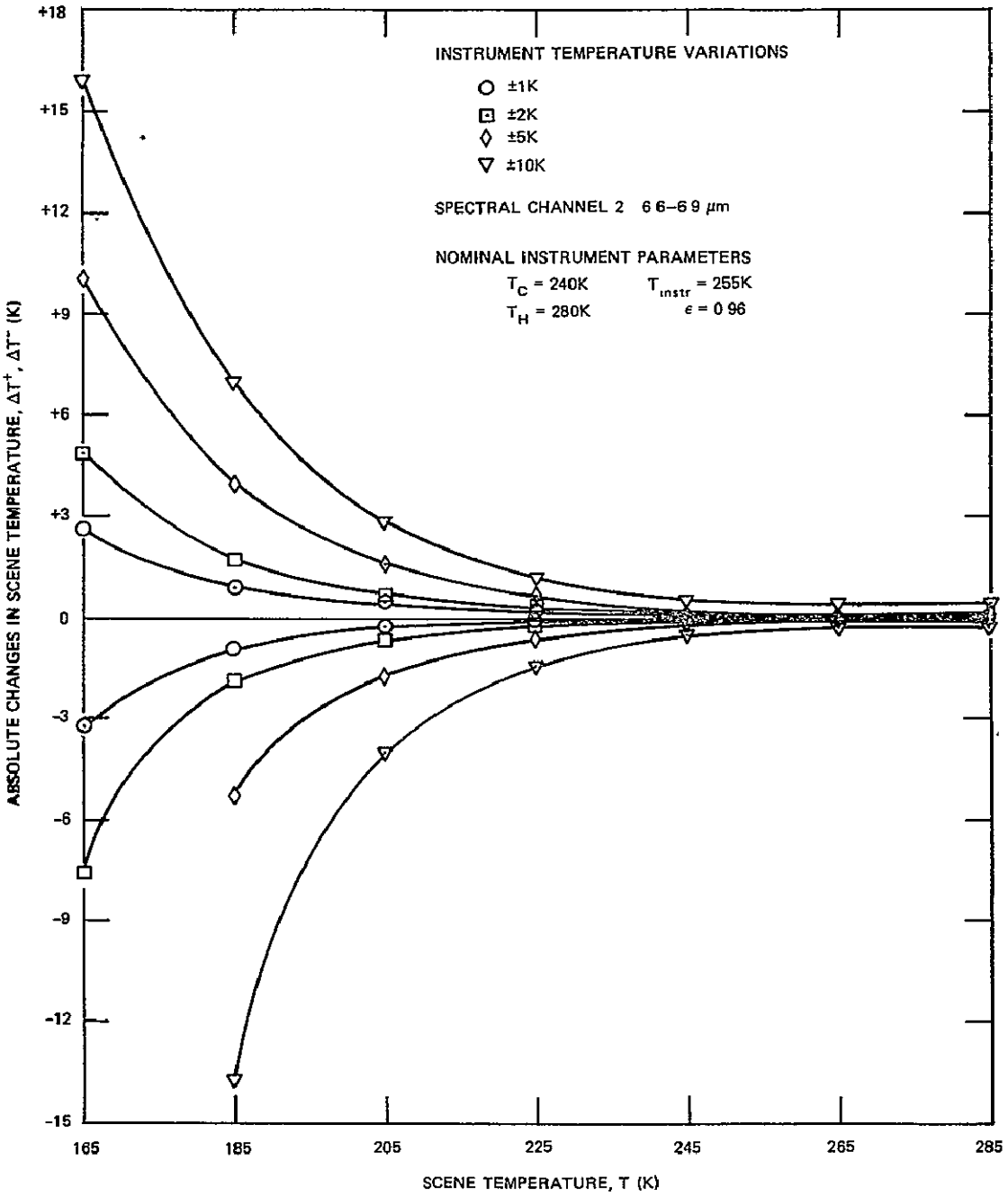

Figure 9. Scene temperature uncertainty curves due to instrument temperature variations about nominal (spectral channel 2) for reduced nominal graybody emissivity

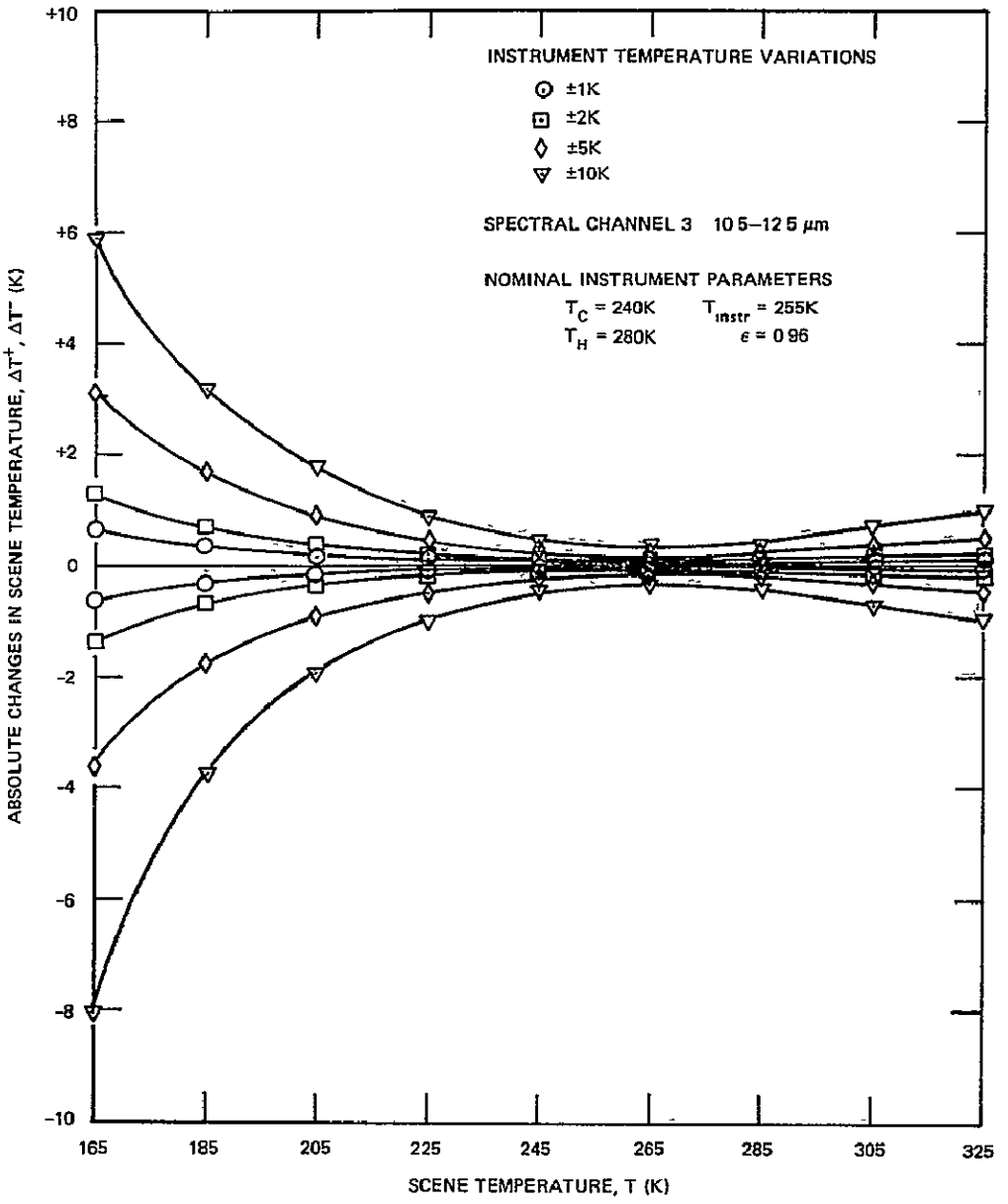

Figure 10. Scene temperature uncertainty curves due to instrument temperature variations about nominal (spectral channel 3) for reduced nominal graybody emissivity

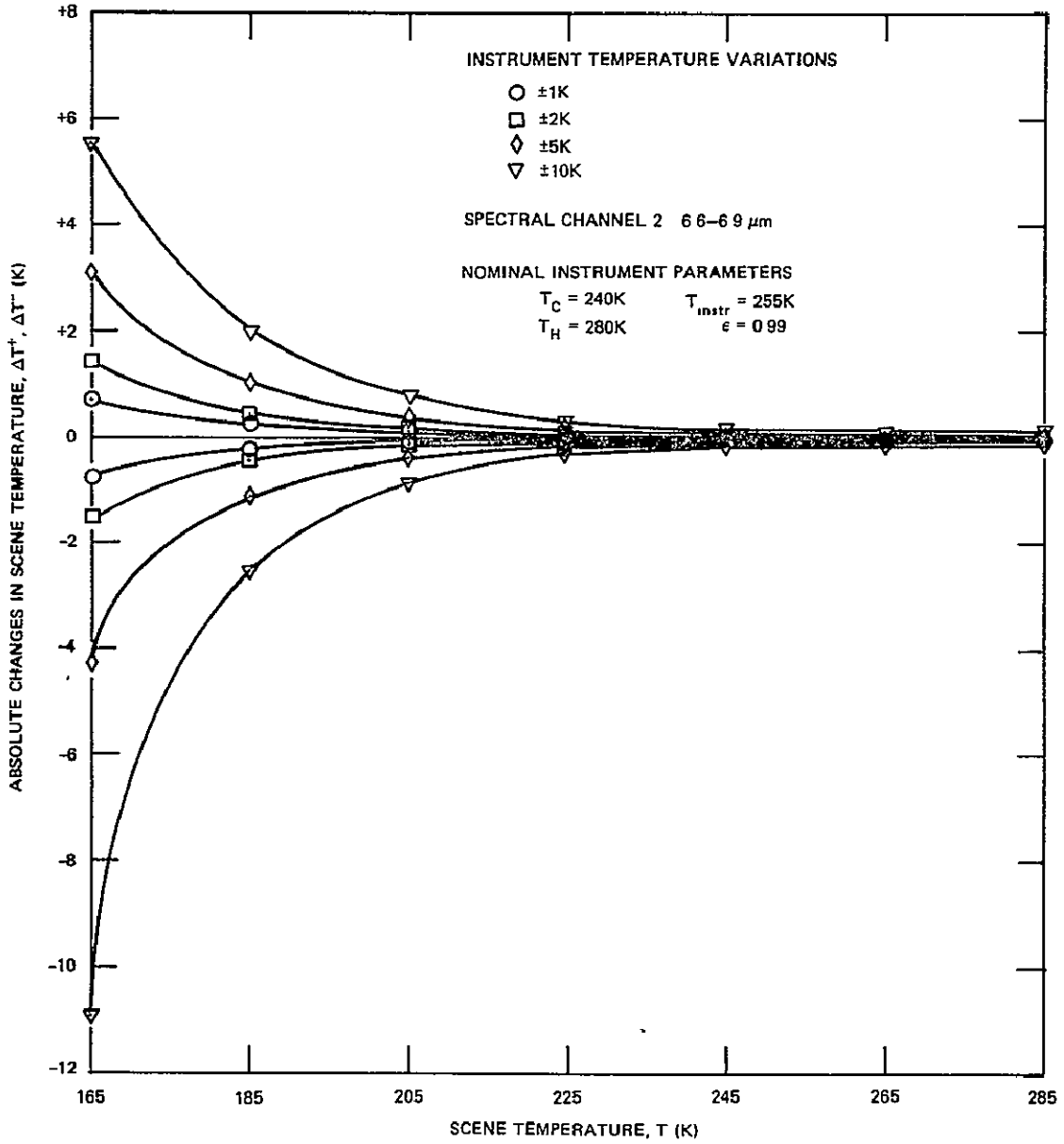

Figure 11. Scene temperature uncertainty curves due to instrument temperature variations about nominal (spectral channel 2) for increased nominal graybody emissivity

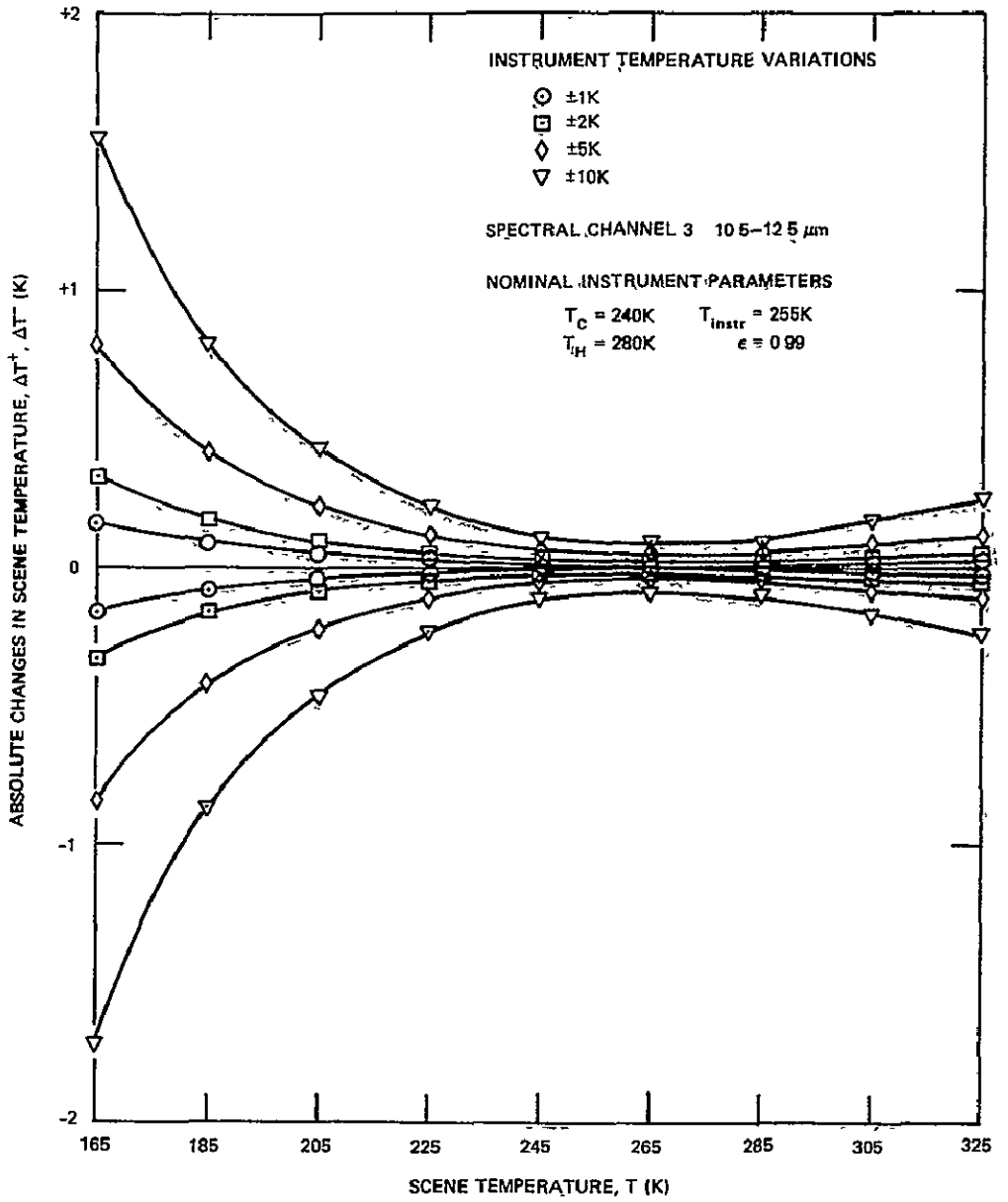

Figure 12. Scene temperature uncertainty curves due to instrument temperature variations about nominal (spectral channel 3) for increased nominal graybody emissivity

scene temperature uncertainty curves for the two spectral channels for each of the "reduced" and "increased" nominal graybody emissivities. These curves will also be discussed in the following section.

DISCUSSION

The results of this parametric error analysis are clearly shown in the scene temperature uncertainty curves (Figures 3 through 8). These curves were determined by using a full range of assumed uncertainty levels (19) in the three parameters, T_{cal}, ϵ, and T_{instr}, from extremely small values to values larger than actually anticipated based upon the specifications and data relating to the C.T.S. radiometer [Refs. 3, 4]. It is obvious from these uncertainty curves that the best calibration accuracies are obtained for scene temperatures in the range between the two graybody calibration target temperatures, viz., 240 K and 280 K. Outside this range, the calibration uncertainties become progressively more severe, particularly for low scene temperatures.* At a scene temperature of 165 K, even the lower sets of uncertainty levels in the radiometer parameters result in calibration temperature errors of several K. For the chosen range of uncertainty levels (19) in the three parameters, the largest uncertainties in scene temperature are produced by variations in the graybody calibration target temperatures, T_C and T_H, and the smallest uncertainties are produced by variations in the instrument temperature, T_{instr}, with variations in graybody emissivities, ϵ, producing scene temperature uncertainties of intermediate magnitudes.

*The omission of certain data points at low scene temperatures from the uncertainty curves of spectral channel 2 results from a type of numerical divergence experienced, which is more fully explained in Appendix A.

For a given scene temperature and a given set of parameter uncertainty levels, the curves in Figures 3 through 8 (or, for greater precision, the tables in Appendix A) can be used to determine the total root-sum-square (R.S.S.) temperature calibration error of the radiometer infrared spectral channels. (Errors due to sources other than uncertainties in the parameters mentioned above, e.g., registration and signal to noise ratio, are not included in this analysis.) As an example, for a 185 K blackbody scene, the calibration uncertainties in spectral channel 2 are as follows (using mean values of the magnitudes of the positive and negative uncertainties): ±3.92 K due to an uncertainty of ±0.2 K in the calibration target temperatures, ±1.86 K due to an uncertainty of ±0.005 in the calibration target emissivities, and ±0.88 K due to an uncertainty of ±2 K in the instrument temperature. The R.S.S. total calibration error is then ±4.43 K for a 185 K blackbody scene in spectral channel 2. An analogous calculation, using the same parameter uncertainty levels, for spectral channel 3 yields an R.S.S. total calibration error of ±1.79 K for a 185 K blackbody scene.

It is possible that the nominal value of the graybody calibration target emissivity could be significantly higher (in accord with a manufacturer's claim, for instance) or lower (due to degradation effects) than the value of 0.98 included in Table 1 and used in generating the curves in Figures 3 through 8. The nominal value of the calibration target emissivity has a significant relative effect on the calibration radiance contribution from the instrument, i.e., the reflection term, as given in equation (4). Therefore, the effects of different nominal values of

the emissivity were studied by recalculating the uncertainty curves due to variations in the instrument temperature parameter only. The "reduced" and "increased" nominal graybody emissivity values of 0.96 and 0.99, respectively, represent reasonable extremes of calibration target emissivities for an aircraft-borne instrument. The results for $\epsilon = 0.96$, given in Figures 9 and 10 for the two infrared spectral channels, show temperature errors of approximately double the magnitude, uniformly for all scene temperatures, of the curves in Figures 5 and 8, respectively, for $\epsilon = 0.98$. The results for $\epsilon = 0.99$, given in Figures 11 and 12 for the two spectral channels, show temperature errors of approximately half the magnitude, uniformly for all scene temperatures, of the curves in Figures 5 and 8, respectively. Thus, the relative magnitudes of the calibration temperature errors due to uncertainties in the instrument temperature are approximately proportional to $(1 - \epsilon)$, the factor in the reflection term of equation (4).

The numerical results provided in this paper are based upon instrument parameters characteristic of the particular case of the C.T.S. radiometer; however, the methods described herein are quite general and the computer programs developed (available upon request to the authors) can be used to model the calibration accuracy of any infrared radiometer.

PAGE INTENTIONALLY BLANK

REFERENCES

1. Carnahan, Brice, Luther, H. A., and Wilkes, James O., Applied Numerical Methods, John Wiley & Sons, New York, 1969.

2. Ostrowski, A. M., Solution of Equations and Systems of Equations, Academic Press, New York and London, 1960.

3. Brown, Kenneth, Specification for Cloud Top Scanning Radiometer (CTS) for a High Altitude Aircraft, Document No. S-944-2, Goddard Space Flight Center, June 1974.

4. Brown, Kenneth, NASA/Goddard Space Flight Center, Private communication, 1977.

PAGE INTENTIONALLY BLANK

APPENDIX A: TABULATION OF RADIANCE AND TEMPERATURE VARIATIONS

The radiance and temperature variations included in Tables A1 through A24 comprise the full set of results for 12 pairs of calibration envelopes for each of the two infrared spectral channels. These calibration envelopes correspond to assumed uncertainties in the nominal values of the graybody calibration target temperatures and emissivities and of the instrument case temperature, as listed in the relations (19). For each scene temperature T, the corresponding scene projected radiance N, calculated by equation (3) and assuming a blackbody target ($\epsilon = 1$), is given. The center two columns provide the corresponding low and high projected radiances, N^- and N^+, given by equations (13), as well as their relative changes from nominal, given by equations (14). The final two columns include the low and high temperatures, T^- and T^+, obtained in equations (17) and (16), respectively, as well as the absolute changes from nominal.

In certain tables, data are replaced by dashes, indicating that a type of divergence has occurred for the given parameter values. Notice that the physical limitation that the low projected radiance $N^- > 0$ is not present in the defining equation (13b). When the lower calibration envelope diverges sufficiently from the nominal calibration curve, a large relative change in the scene projected radiance (most likely, at a low scene temperature) can mathematically produce $N^- \leq 0$ by equation (13b). Such a condition, indicated by the dashes in the tables, occurs only when the corresponding relative change in the high projected radiance

exceeds unity (or nearly so, since the symmetry between upper and lower calibration envelopes is only approximate). This condition occurs only for the lower scene temperatures in spectral channel 2, since larger scene radiances are present in spectral channel 3 even at the lowest scene temperatures.

NOTE: In Tables A1 through A24, all projected radiance parameters are given in units of ergs/cm^2-sec-sterad, and all temperatures (including absolute changes in temperature) are in units of K. The relative changes in projected radiances are dimensionless.

Table A1
Radiance and Temperature Variations in Spectral Channel 2
due to $\Delta T = \pm 0.1$ K Uncertainties

Scene Temperature, T	Scene Projected Radiance, N	Low Projected Radiance, N^-	High Projected Radiance, N^+	Low Temperature, T^-	High Temperature, T^+
		Relative Change, $\Delta N^-/N$	Relative Change, $\Delta N^+/N$	Absolute Change, ΔT^-	Absolute Change, ΔT^+
165	6.273	3.124 -0.5019	9.386 0.4963	156.54 -8.46	170.32 5.32
185	25.316	22.268 -0.1204	28.330 0.1191	182.96 -2.04	186.83 1.83
205	77.840	75.068 -0.0356	80.581 0.0352	204.29 -0.71	205.68 0.68
225	196.052	193.902 -0.0110	198.178 0.0108	224.74 -0.26	225.26 0.26
245	424.729	423.292 -0.0034	426.168 0.0034	244.90 -0.10	245.10 0.10
265	818.919	816.564 -0.0029	821.281 0.0029	264.91 -0.09	265.09 0.09
285	1440.208	1435.857 -0.0030	1444.597 0.0030	284.88 -0.12	285.12 0.12

Table A2
Radiance and Temperature Variations in Spectral Channel 2
due to $\Delta T = \pm 0.2$ K Uncertainties

Scene Temperature, T	Scene Projected Radiance, N	Low Projected Radiance, N^-	High Projected Radiance, N^+	Low Temperature, T^-	High Temperature, T^+
		Relative Change, $\Delta N^-/N$	Relative Change, $\Delta N^+/N$	Absolute Change, ΔT^-	Absolute Change, ΔT^+
165	6.273	–	12.464	–	174.27
		–	0.9870	–	9.27
185	25.316	19.185	31.310	180.65	188.48
		-0.2422	0.2368	-4.35	3.48
205	77.840	72.264	83.291	203.54	206.34
		-0.0716	0.0700	-1.46	1.34
225	196.052	191.725	200.278	224.47	225.51
		-0.0221	0.0216	-0.53	0.51
245	424.729	421.859	427.610	244.81	245.19
		-0.0068	0.0068	-0.19	0.19
265	818.919	814.214	823.648	264.81	265.19
		-0.0057	0.0058	-0.19	0.19
285	1440.208	1431.545	1449.025	284.77	285.23
		-0.0060	0.0061	-0.23	0.23

Table A3
Radiance and Temperature Variations in Spectral Channel 2
due to $\Delta T = \pm 0.5$ K Uncertainties

Scene Temperature, T	Scene Projected Radiance, N	Low Projected Radiance, N^-	High Projected Radiance, N^+	Low Temperature, T^-	High Temperature, T^+
		Relative Change, $\Delta N^-/N$	Relative Change, $\Delta N^+/N$	Absolute Change, ΔT^-	Absolute Change, ΔT^+
165	6.273	–	21.497	–	182.41
		–	2.4270	–	17.41
185	25.316	9.722	40.054	170.80	192.68
		-0.6160	0.5821	-14.20	7.68
205	77.840	63.654	91.237	201.11	208.18
		-0.1822	0.1721	-3.89	3.18
225	196.052	185.036	206.432	223.63	226.23
		-0.0562	0.0529	-1.37	1.23
245	424.729	417.575	431.953	244.52	245.48
		-0.0168	0.0170	-0.48	0.48
265	818.919	807.198	830.785	264.53	265.47
		-0.0143	0.0145	-0.47	0.47
285	1440.208	1418.827	1462.548	284.43	285.59
		-0.0148	0.0155	-0.57	0.59

Table A4
Radiance and Temperature Variations in Spectral Channel 2
due to $\Delta T = \pm 1.0$ K Uncertainties

Scene Temperature, T	Scene Projected Radiance, N	Low Projected Radiance, N^-	High Projected Radiance, N^+	Low Temperature, T^-	High Temperature, T^+
		Relative Change, $\Delta N^-/N$	Relative Change, $\Delta N^+/N$	Absolute Change, ΔT^-	Absolute Change, ΔT^+
165	6.273	–	35.903	–	190.79
		–	4.7236	–	25.79
185	25.316	–	53.997	–	198.03
		–	1.1329	–	13.03
205	77.840	48.616	103.902	196.12	210.86
		-0.3754	0.3348	-8.88	5.86
225	196.052	173.330	216.219	222.11	227.35
		-0.1159	0.1029	-2.89	2.35
245	424.729	410.490	439.248	244.04	245.95
		-0.0335	0.0342	-0.96	0.95
265	818.919	795.617	842.797	264.05	265.95
		-0.0285	0.0292	-0.95	0.95
285	1440.208	1398.336	1485.920	283.88	286.20
		-0.0291	0.0317	-1.12	1.20

Table A5
Radiance and Temperature Variations in Spectral Channel 2
due to $\Delta\epsilon = \pm 0.001$ Uncertainties

Scene Temperature, T	Scene Projected Radiance, N	Low Projected Radiance, N^-	High Projected Radiance, N^+	Low Temperature, T^-	High Temperature, T^+
		Relative Change, $\Delta N^-/N$	Relative Change, $\Delta N^+/N$	Absolute Change, ΔT^-	Absolute Change, ΔT^+
165	6.273	5.669 -0.0963	6.875 0.0961	163.72 -1.28	166.18 1.18
185	25.316	24.732 -0.0231	25.899 0.0230	184.63 -0.37	185.37 0.37
205	77.840	77.310 -0.0068	78.370 0.0068	204.87 -0.13	205.13 0.13
225	196.052	195.642 -0.0021	196.461 0.0021	224.95 -0.05	225.05 0.05
245	424.729	424.455 -0.0006	425.003 0.0006	244.98 -0.02	245.02 0.02
265	818.919	818.459 -0.0006	819.380 0.0006	264.98 -0.02	265.02 0.02
285	1440.208	1439.349 -0.0006	1441.069 0.0006	284.98 -0.02	285.02 0.02

Table A6
Radiance and Temperature Variations in Spectral Channel 2
due to $\Delta\epsilon = \pm 0.005$ Uncertainties

Scene Temperature, T	Scene Projected Radiance, N	Low Projected Radiance, N^-	High Projected Radiance, N^+	Low Temperature, T^-	High Temperature, T^+
		Relative Change, $\Delta N^-/N$	Relative Change, $\Delta N^+/N$	Absolute Change, ΔT^-	Absolute Change, ΔT^+
165	6.273	3.241 -0.4833	9.273 0.4783	156.97 -8.03	170.15 5.15
185	25.316	22.382 -0.1159	28.220 0.1147	183.04 -1.96	186.76 1.76
205	77.840	75.176 -0.0342	80.478 0.0339	204.32 -0.68	205.66 0.66
225	196.052	193.994 -0.0105	198.090 0.0104	224.75 -0.25	225.25 0.25
245	424.729	423.362 -0.0032	426.102 0.0032	244.91 -0.09	245.09 0.09
265	818.919	816.623 -0.0028	821.227 0.0028	264.91 -0.09	265.09 0.09
285	1440.208	1435.930 -0.0030	1444.530 0.0030	284.89 -0.11	285.11 0.11

Table A7
Radiance and Temperature Variations in Spectral Channel 2
due to $\Delta\epsilon = \pm 0.01$ Uncertainties

Scene Temperature, T	Scene Projected Radiance, N	Low Projected Radiance, N^-	High Projected Radiance, N^+	Low Temperature, T^-	High Temperature, T^+
		Relative Change, $\Delta N^-/N$	Relative Change, $\Delta N^+/N$	Absolute Change, ΔT^-	Absolute Change, ΔT^+
165	6.273	0.179	12.244	129.33	174.02
		-0.9715	0.9519	-35.67	9.02
185	25.316	19.418	31.095	180.83	188.36
		-0.2330	0.2283	-4.17	3.36
205	77.840	72.484	83.088	203.60	206.30
		-0.0688	0.0674	-1.40	1.30
225	196.052	191.915	200.106	224.49	225.49
		-0.0211	0.0207	-0.51	0.49
245	424.729	422.001	427.482	244.82	245.18
		-0.0064	0.0065	-0.18	0.18
265	818.919	814.337	823.545	264.82	265.19
		-0.0056	0.0056	-0.18	0.19
285	1440.208	1431.695	1448.897	284.77	285.23
		-0.0059	0.0060	-0.23	0.23

Table A8
Radiance and Temperature Variations in Spectral Channel 2
due to $\Delta\epsilon = \pm 0.02$ Uncertainties

Scene Temperature, T	Scene Projected Radiance, N	Low Projected Radiance, N^-	High Projected Radiance, N^+	Low Temperature, T^-	High Temperature, T^+
		Relative Change, $\Delta N^-/N$	Relative Change, $\Delta N^+/N$	Absolute Change, ΔT^-	Absolute Change, ΔT^+
165	6.273	–	18.095	–	179.76
		–	1.8847	–	14.76
185	25.316	13.398	36.758	175.31	191.19
		-0.4708	0.4519	-9.69	6.19
205	77.840	67.016	88.231	202.09	207.50
		-0.1391	0.1335	-2.91	2.50
225	196.052	187.691	204.079	223.97	225.96
		-0.0426	0.0409	-1.03	0.96
245	424.729	419.299	430.262	244.64	245.37
		-0.0128	0.0130	-0.36	0.37
265	818.919	809.798	828.215	264.63	265.37
		-0.0111	0.0114	-0.37	0.37
285	1440.208	1423.352	1457.767	284.55	285.46
		-0.0117	0.0122	-0.45	0.46

Table A9
Radiance and Temperature Variations in Spectral Channel 2
due to $\Delta T_{instr} = \pm 1$ K Uncertainties

Scene Temperature, T	Scene Projected Radiance, N	Low Projected Radiance, N^-	High Projected Radiance, N^+	Low Temperature, T^-	High Temperature, T^+
		Relative Change, $\Delta N^-/N$	Relative Change, $\Delta N^+/N$	Absolute Change, ΔT^-	Absolute Change, ΔT^+
165	6.273	5.564	6.970	163.48	166.36
		-0.1130	0.1112	-1.52	1.36
185	25.316	24.624	25.997	184.56	185.43
		-0.0273	0.0269	-0.44	0.43
205	77.840	77.195	78.475	204.84	205.16
		-0.0083	0.0082	-0.16	0.16
225	196.052	195.511	196.583	224.93	225.06
		-0.0028	0.0027	-0.07	0.06
245	424.729	424.332	425.115	244.97	245.03
		-0.0009	0.0009	-0.03	0.03
265	818.919	818.523	819.306	264.98	265.02
		-0.0005	0.0005	-0.02	0.02
285	1440.208	1439.641	1440.766	284.99	285.01
		-0.0004	0.0004	-0.01	0.01

Table A10
Radiance and Temperature Variations in Spectral Channel 2
due to $\Delta T_{instr} = \pm 2$ K Uncertainties

Scene Temperature, T	Scene Projected Radiance, N	Low Projected Radiance, N^-	High Projected Radiance, N^+	Low Temperature, T^-	High Temperature, T^+
		Relative Change, $\Delta N^-/N$	Relative Change, $\Delta N^+/N$	Absolute Change, ΔT^-	Absolute Change, ΔT^+
165	6.273	4.844	7.657	161.76	167.59
		-0.2277	0.2207	-3.24	2.59
185	25.316	23.921	26.667	184.09	185.84
		-0.0551	0.0534	-0.91	0.84
205	77.840	76.538	79.099	204.67	205.32
		-0.0167	0.0162	-0.33	0.32
225	196.052	194.960	197.102	224.87	225.13
		-0.0056	0.0054	-0.13	0.13
245	424.729	423.926	425.493	244.95	245.05
		-0.0019	0.0018	-0.05	0.05
265	818.919	818.116	819.683	264.97	265.03
		-0.0010	0.0009	-0.03	0.03
285	1440.208	1439.066	1441.315	284.97	285.03
		-0.0008	0.0008	-0.03	0.03

Table A11
Radiance and Temperature Variations in Spectral Channel 2
due to ΔT_{instr} = ±5 K Uncertainties

Scene Temperature, T	Scene Projected Radiance, N	Low Projected Radiance, N^-	High Projected Radiance, N^+	Low Temperature, T^-	High Temperature, T^+
		Relative Change, $\Delta N^-/N$	Relative Change, $\Delta N^+/N$	Absolute Change, ΔT^-	Absolute Change, ΔT^+
165	6.273	2.614 -0.5833	9.657 0.5394	154.52 -10.48	170.71 5.71
185	25.316	21.741 -0.1412	28.616 0.1304	182.59 -2.41	186.99 1.99
205	77.840	74.499 -0.0429	80.909 0.0394	204.14 -0.86	205.77 0.77
225	196.052	193.236 -0.0144	198.601 0.0130	224.66 -0.34	225.31 0.31
245	424.729	422.645 -0.0049	426.568 0.0043	244.86 -0.14	245.12 0.12
265	818.919	816.836 -0.0025	820.758 0.0022	264.92 -0.08	265.07 0.07
285	1440.208	1437.283 -0.0020	1442.914 0.0019	284.92 -0.08	285.07 0.07

Table A12
Radiance and Temperature Variations in Spectral Channel 2
due to $\Delta T_{instr} = \pm 10$ K Uncertainties

Scene Temperature, T	Scene Projected Radiance, N	Low Projected Radiance, N^-	High Projected Radiance, N^+	Low Temperature, T^-	High Temperature, T^+
		Relative Change, $\Delta N^-/N$	Relative Change, $\Delta N^+/N$	Absolute Change, ΔT^-	Absolute Change, ΔT^+
165	6.273	–	12.803	–	174.66
		–	1.0410	–	9.66
185	25.316	17.854	31.678	179.55	188.67
		-0.2948	0.2513	-5.45	3.67
205	77.840	70.849	83.740	203.16	206.45
		-0.0898	0.0758	-1.84	1.45
225	196.052	190.120	200.911	224.27	225.58
		-0.0303	0.0248	-0.73	0.58
245	424.729	420.298	428.182	244.71	245.23
		-0.0104	0.0081	-0.29	0.23
265	818.919	814.489	822.372	264.82	265.14
		-0.0054	0.0042	-0.18	0.14
285	1440.208	1434.114	1445.425	284.84	285.14
		-0.0042	0.0036	-0.16	0.14

Table A13
Radiance and Temperature Variations in Spectral Channel 3
due to $\Delta T = \pm 0.1$ K Uncertainties

Scene Temperature, T	Scene Projected Radiance, N	Low Projected Radiance, N^-	High Projected Radiance, N^+	Low Temperature, T^-	High Temperature, T^+
		Relative Change, $\Delta N^-/N$	Relative Change, $\Delta N^+/N$	Absolute Change, ΔT^-	Absolute Change, ΔT^+
165	600.727	557.192	643.811	163.37	166.53
		-0.0725	0.0717	-1.63	1.53
185	1361.220	1321.515	1400.511	184.19	185.78
		-0.0292	0.0289	-0.81	0.78
205	2634.122	2600.827	2667.066	204.57	205.42
		-0.0126	0.0125	-0.43	0.42
225	4539.862	4516.165	4563.303	224.79	225.21
		-0.0052	0.0052	-0.21	0.21
245	7169.241	7154.676	7183.819	244.90	245.10
		-0.0020	0.0020	-0.10	0.10
265	10581.566	10563.202	10599.952	264.90	265.10
		-0.0017	0.0017	-0.10	0.10
285	14807.538	14779.782	14835.552	284.88	285.12
		-0.0019	0.0019	-0.12	0.12
305	19854.296	19801.377	19907.728	304.81	305.20
		-0.0027	0.0027	-0.19	0.20
325	25710.952	25628.829	25793.879	324.74	325.27
		-0.0032	0.0032	-0.26	0.27

Table A14
Radiance and Temperature Variations in Spectral Channel 3
due to $\Delta T = \pm 0.2$ K Uncertainties

Scene Temperature, T	Scene Projected Radiance, N	Low Projected Radiance, N^-	High Projected Radiance, N^+	Low Temperature, T^-	High Temperature, T^+
		Relative Change, $\Delta N^-/N$	Relative Change, $\Delta N^+/N$	Absolute Change, ΔT^-	Absolute Change, ΔT^+
165	600.727	513.198 -0.1457	686.448 0.1427	161.63 -3.37	167.96 2.96
185	1361.220	1281.390 -0.0586	1439.394 0.0574	183.36 -1.64	186.54 1.54
205	2634.122	2567.177 -0.0254	2699.665 0.0249	204.14 -0.86	205.83 0.83
225	4539.862	4492.210 -0.0105	4586.494 0.0103	224.58 -0.42	225.41 0.41
245	7169.241	7140.124 -0.0041	7198.411 0.0041	244.81 -0.19	245.19 0.19
265	10581.566	10544.858 -0.0035	10618.359 0.0035	264.81 -0.19	265.19 0.19
285	14807.538	14752.282 -0.0037	14863.829 0.0038	284.76 -0.24	285.24 0.24
305	19854.296	19748.961 -0.0053	19961.679 0.0054	304.61 -0.39	305.39 0.39
325	25710.952	25547.500 -0.0064	25877.623 0.0065	324.48 -0.52	325.53 0.53

Table A15
Radiance and Temperature Variations in Spectral Channel 3
due to $\Delta T = \pm 0.5$ K Uncertainties

Scene Temperature, T	Scene Projected Radiance, N	Low Projected Radiance, N^-	High Projected Radiance, N^+	Low Temperature, T^-	High Temperature, T^+
		Relative Change, $\Delta N^-/N$	Relative Change, $\Delta N^+/N$	Absolute Change, ΔT^-	Absolute Change, ΔT^+
165	600.727	378.393	811.755	155.48	171.84
		-0.3701	0.3513	-9.52	6.84
185	1361.220	1158.428	1553.657	180.69	188.69
		-0.1490	0.1414	-4.31	3.69
205	2634.122	2464.040	2795.443	202.79	207.01
		-0.0646	0.0612	-2.21	2.01
225	4539.862	4418.752	4654.597	223.92	226.01
		-0.0267	0.0253	-1.08	1.01
245	7169.241	7096.549	7242.268	244.52	245.48
		-0.0101	0.0102	-0.48	0.48
265	10581.566	10489.955	10673.710	264.52	265.48
		-0.0087	0.0087	-0.48	0.48
285	14807.538	14671.276	14950.280	284.41	285.61
		-0.0092	0.0096	-0.59	0.61
305	19854.296	19594.666	20126.728	304.04	306.00
		-0.0131	0.0137	-0.96	1.00
325	25710.952	25308.154	26133.884	323.71	326.35
		-0.0157	0.0164	-1.29	1.35

Table A16
Radiance and Temperature Variations in Spectral Channel 3
due to $\Delta T = \pm 1.0$ K Uncertainties

Scene Temperature, T	Scene Projected Radiance, N	Low Projected Radiance, N^-	High Projected Radiance, N^+	Low Temperature, T^-	High Temperature, T^+
		Relative Change, $\Delta N^-/N$	Relative Change, $\Delta N^+/N$	Absolute Change, ΔT^-	Absolute Change, ΔT^+
165	600.727	143.857	1012.285	138.71	177.23
		-0.7605	0.6851	-26.29	12.23
185	1361.220	944.463	1736.480	175.50	191.91
		-0.3062	0.2757	-9.50	6.91
205	2634.122	2284.505	2948.629	200.33	208.85
		-0.1327	0.1194	-4.67	3.85
225	4539.862	4290.764	4763.412	222.75	226.95
		-0.0549	0.0492	-2.25	1.95
245	7169.241	7024.188	7315.635	244.03	245.97
		-0.0202	0.0204	-0.97	0.97
265	10581.566	10398.869	10766.395	264.04	265.96
		-0.0173	0.0175	-0.96	0.96
285	14807.538	14541.034	15100.016	283.84	286.25
		-0.0180	0.0198	-1.16	1.25
305	19854.296	19346.922	20412.970	303.13	307.03
		-0.0256	0.0281	-1.87	2.03
325	25710.952	24924.052	26578.539	322.46	327.75
		-0.0306	0.0337	-2.54	2.75

Table A17
Radiance and Temperature Variations in Spectral Channel 3
due to $\Delta\epsilon = \pm 0.001$ Uncertainties

Scene Temperature, T	Scene Projected Radiance, N	Low Projected Radiance, N^-	High Projected Radiance, N^+	Low Temperature, T^-	High Temperature, T^+
		Relative Change, $\Delta N^-/N$	Relative Change, $\Delta N^+/N$	Absolute Change, ΔT^-	Absolute Change, ΔT^+
165	600.727	592.378	609.060	164.69	165.30
		-0.0139	0.0139	-0.31	0.30
185	1361.220	1353.647	1368.777	184.85	185.15
		-0.0056	0.0056	-0.15	0.15
205	2634.122	2627.849	2640.382	204.92	205.08
		-0.0024	0.0024	-0.08	0.08
225	4539.862	4535.536	4544.179	224.96	225.04
		-0.0010	0.0010	-0.04	0.04
245	7169.241	7166.660	7171.823	244.98	245.02
		-0.0004	0.0004	-0.02	0.02
265	10581.566	10577.752	10585.383	264.98	265.02
		-0.0004	0.0004	-0.02	0.02
285	14807.538	14801.388	14813.700	284.97	285.03
		-0.0004	0.0004	-0.03	0.03
305	19854.296	19843.002	19865.613	304.96	305.04
		-0.0006	0.0006	-0.04	0.04
325	25710.952	25693.688	25728.251	324.94	325.06
		-0.0007	0.0007	-0.06	0.06

Table A18
Radiance and Temperature Variations in Spectral Channel 3
due to $\Delta\epsilon = \pm 0.005$ Uncertainties

Scene Temperature, T	Scene Projected Radiance, N	Low Projected Radiance, N^-	High Projected Radiance, N^+	Low Temperature, T^-	High Temperature, T^+
		Relative Change, $\Delta N^-/N$	Relative Change, $\Delta N^+/N$	Absolute Change, ΔT^-	Absolute Change, ΔT^+
165	600.727	558.808 -0.0698	642.221 0.0691	163.44 -1.56	166.47 1.47
185	1361.220	1323.201 -0.0279	1398.853 0.0276	184.23 -0.77	185.75 0.75
205	2634.122	2602.630 -0.0120	2665.294 0.0118	204.60 -0.40	205.40 0.40
225	4539.862	4518.143 -0.0048	4561.360 0.0047	224.81 -0.19	225.19 0.19
245	7169.241	7156.356 -0.0018	7182.171 0.0018	244.91 -0.09	245.09 0.09
265	10581.566	10562.521 -0.0018	10600.680 0.0018	264.90 -0.10	265.10 0.10
285	14807.538	14776.916 -0.0021	14838.474 0.0021	284.87 -0.13	285.13 0.13
305	19854.296	19798.056 -0.0028	19911.113 0.0029	304.79 -0.21	305.21 0.21
325	25710.952	25624.982 -0.0033	25797.803 0.0034	324.72 -0.28	325.28 0.28

Table A19
Radiance and Temperature Variations in Spectral Channel 3
due to $\Delta\epsilon = \pm 0.01$ Uncertainties

Scene Temperature, T	Scene Projected Radiance, N	Low Projected Radiance, N^-	High Projected Radiance, N^+	Low Temperature, T^-	High Temperature, T^+
		Relative Change, $\Delta N^-/N$	Relative Change, $\Delta N^+/N$	Absolute Change, ΔT^-	Absolute Change, ΔT^+
165	600.727	516.457	683.296	161.76	167.86
		-0.1403	0.1374	-3.24	2.86
185	1361.220	1284.789	1436.107	183.43	186.48
		-0.0561	0.0550	-1.57	1.48
205	2634.122	2570.814	2696.151	204.19	205.78
		-0.0240	0.0235	-0.81	0.78
225	4539.862	4496.201	4582.641	224.61	225.38
		-0.0096	0.0094	-0.39	0.38
245	7169.241	7143.519	7195.149	244.83	245.17
		-0.0036	0.0036	-0.17	0.17
265	10581.566	10543.545	10619.863	264.80	265.20
		-0.0036	0.0036	-0.20	0.20
285	14807.538	14746.603	14869.729	284.74	285.27
		-0.0041	0.0042	-0.26	0.27
305	19854.296	19742.384	19968.516	304.59	305.42
		-0.0056	0.0058	-0.41	0.42
325	25710.952	25539.881	25885.549	324.45	325.56
		-0.0067	0.0068	-0.55	0.56

Table A20
Radiance and Temperature Variations in Spectral Channel 3
due to $\Delta\epsilon = \pm 0.02$ Uncertainties

Scene Temperature, T	Scene Projected Radiance, N	Low Projected Radiance, N^-	High Projected Radiance, N^+	Low Temperature, T^-	High Temperature, T^+
		Relative Change, $\Delta N^-/N$	Relative Change, $\Delta N^+/N$	Absolute Change, ΔT^-	Absolute Change, ΔT^+
165	600.727	430.430 -0.2835	764.213 0.2721	158.03 -6.97	170.43 5.43
185	1361.220	1206.766 -0.1135	1509.496 0.1089	181.76 -3.24	187.87 2.87
205	2634.122	2506.187 -0.0486	2756.939 0.0466	203.34 -1.66	206.54 1.54
225	4539.862	4451.630 -0.0194	4624.565 0.0187	224.21 -0.79	225.75 0.75
245	7169.241	7117.981 -0.0071	7221.247 0.0073	244.66 -0.34	245.34 0.34
265	10581.566	10505.798 -0.0072	10658.439 0.0073	264.60 -0.40	265.40 0.40
285	14807.538	14686.887 -0.0081	14933.215 0.0085	284.48 -0.52	285.54 0.54
305	19854.296	19632.710 -0.0112	20085.115 0.0116	304.19 -0.81	305.84 0.84
325	25710.952	25372.233 -0.0132	26063.784 0.0137	323.91 -1.09	326.12 1.12

Table A21
Radiance and Temperature Variations in Spectral Channel 3
due to $\Delta T_{instr} = \pm 1$ K Uncertainties

Scene Temperature, T	Scene Projected Radiance, N	Low Projected Radiance, N^-	High Projected Radiance, N^+	Low Temperature, T^-	High Temperature, T^+
		Relative Change, $\Delta N^-/N$	Relative Change, $\Delta N^+/N$	Absolute Change, ΔT^-	Absolute Change, ΔT^+
165	600.727	591.623	609.774	164.67	165.33
		-0.0152	0.0151	-0.33	0.33
185	1361.220	1352.848	1369.536	184.83	185.17
		-0.0062	0.0061	-0.17	0.17
205	2634.122	2626.976	2641.214	204.91	205.09
		-0.0027	0.0027	-0.09	0.09
225	4539.862	4534.552	4545.122	224.95	225.05
		-0.0012	0.0012	-0.05	0.05
245	7169.241	7165.809	7172.632	244.98	245.02
		-0.0005	0.0005	-0.02	0.02
265	10581.566	10578.135	10584.957	264.98	265.02
		-0.0003	0.0003	-0.02	0.02
285	14807.538	14802.926	14812.118	284.98	285.02
		-0.0003	0.0003	-0.02	0.02
305	19854.296	19844.832	19863.738	304.97	305.03
		-0.0005	0.0005	-0.03	0.03
325	25710.952	25695.857	25726.035	324.95	325.05
		-0.0006	0.0006	-0.05	0.05

Table A22
Radiance and Temperature Variations in Spectral Channel 3
due to $\Delta T_{instr} = \pm 2$ K Uncertainties

Scene Temperature, T	Scene Projected Radiance, N	Low Projected Radiance, N^-	High Projected Radiance, N^+	Low Temperature, T^-	High Temperature, T^+
		Relative Change, $\Delta N^-/N$	Relative Change, $\Delta N^+/N$	Absolute Change, ΔT^-	Absolute Change, ΔT^+
165	600.727	582.460	618.764	164.33	165.65
		-0.0304	0.0300	-0.67	0.65
185	1361.220	1344.419	1377.796	184.66	185.33
		-0.0123	0.0122	-0.34	0.33
205	2634.122	2619.776	2648.252	204.82	205.18
		-0.0054	0.0054	-0.18	0.18
225	4539.862	4529.191	4550.331	224.91	225.09
		-0.0024	0.0023	-0.09	0 09
245	7169.241	7162.338	7175.982	244.95	245.04
		-0.0010	0.0009	-0.05	0.04
265	10581.566	10574.664	10588.308	264.96	265.04
		-0.0007	0.0006	-0.04	0.04
285	14807.538	14798.283	14816.667	284.96	285.04
		-0.0006	0.0006	-0.04	0.04
305	19854.296	19835.346	19873.158	304.93	305.07
		-0.0010	0.0010	-0.07	0.07
325	25710.952	25680.751	25741.108	324.90	325.10
		-0.0012	0.0012	-0.10	0.10

Table A23
Radiance and Temperature Variations in Spectral Channel 3
due to $\Delta T_{instr} = \pm 5$ K Uncertainties

Scene Temperature, T	Scene Projected Radiance, N	Low Projected Radiance, N^-	High Projected Radiance, N^+	Low Temperature, T^-	High Temperature, T^+
		Relative Change, $\Delta N^-/N$	Relative Change, $\Delta N^+/N$	Absolute Change, ΔT^-	Absolute Change, ΔT^+
165	600.727	554.621 -0.0768	645.393 0.0744	163.27 -1.73	166.58 1.58
185	1361.220	1318.790 -0.0312	1402.243 0.0301	184.14 -0.86	185.82 0.82
205	2634.122	2597.847 -0.0138	2669.049 0.0133	204.54 -0.46	205.44 0.44
225	4539.862	4512.802 -0.0060	4565.662 0.0057	224.76 -0.24	225.23 0.23
245	7169.241	7151.681 -0.0024	7185.795 0.0023	244.88 -0.12	245.11 0.11
265	10581.566	10564.007 -0.0017	10598.121 0.0016	264.91 -0.09	265.09 0.09
285	14807.538	14784.165 -0.0016	14830.127 0.0015	284.90 -0.10	285.10 0.10
305	19854.296	19806.754 -0.0024	19901.289 0.0024	304.83 -0.17	305.17 0.17
325	25710.952	25635.361 -0.0029	25786.264 0.0029	324.76 -0.24	325.24 0.24

Table A24
Radiance and Temperature Variations in Spectral Channel 3
due to $\Delta T_{instr} = \pm 10$ K Uncertainties

Scene Temperature, T	Scene Projected Radiance, N	Low Projected Radiance, N^-	High Projected Radiance, N^+	Low Temperature, T^-	High Temperature, T^+
		Relative Change, $\Delta N^-/N$	Relative Change, $\Delta N^+/N$	Absolute Change, ΔT^-	Absolute Change, ΔT^+
165	600.727	507.027 -0.1560	688.663 0.1464	161.38 -3.62	168.04 3.04
185	1361.220	1274.912 -0.0634	1441.904 0.0593	183.22 -1.78	186.59 1.59
205	2634.122	2560.187 -0.0281	2702.669 0.0260	204.05 -0.95	205.86 0.86
225	4539.862	4484.452 -0.0122	4590.237 0.0111	224.51 -0.49	225.45 0.45
245	7169.241	7133.109 -0.0050	7201.356 0.0045	244.76 -0.24	245.21 0.21
265	10581.566	10545.435 -0.0034	10613.681 0.0030	264.81 -0.19	265.17 0.17
285	14807.538	14760.008 -0.0032	14851.936 0.0030	284.79 -0.21	285.19 0.19
305	19854.296	19758.645 -0.0048	19947.752 0.0047	304.65 -0.35	305.34 0.34
325	25710.952	25559.456 -0.0059	25861.338 0.0058	324.51 -0.49	325.48 0.48

APPENDIX B: NUMERICAL DATA ON CONVERGENCE OF ITERATIVE PROCEDURES

In the numerical integration of Planck's function, as indicated in equations (5) and (6), the value adopted throughout this study for 2n, equal to the number of subintervals used in the application of the composite Simpson's rule, is 20. This value for n was found to produce adequate precision and leads to a subinterval length H of 1.5×10^{-6} cm for spectral channel 2 and 1.0×10^{-5} cm for spectral channel 3.

In the iterative method of false position used to calculate T^- and T^+, the nominal temperature T was decreased or increased, respectively, by 10 K (half the interval width of 20 K between successive T values) as an initial (i = 1) approximation in equations (17) and (16), for T^- and T^+, respectively. These initial approximations were generally sufficient to produce convergence within 3 to 15 iterations using pre-selected convergence criteria ϵ^+, ϵ^- of 10^{-5}, as given in equations (18). The few isolated exceptions to this generalization occur at times when either of the absolute changes, ΔT^- or ΔT^+, in the nominal temperature exceed 10 K. These cases, in which more than 15 iterations were required to converge to the 10^{-5} criteria, are as follows:

Table A3 (Channel 2, $\Delta T = \pm 0.5$ K)

T = 165 K	$\Delta T^+ = 17.41$ K	27 iterations

Table A4 (Channel 2, $\Delta T = \pm 1.0$ K)

T = 165 K	$\Delta T^+ = 25.79$ K	81 iterations

Table A7 (Channel 2, $\Delta\epsilon = \pm 0.01$)

T = 165 K	$\Delta T^{-} = -35.67$ K	85 iterations

Table A8 (Channel 2, $\Delta\epsilon = \pm 0.02$)

T = 165 K	$\Delta T^{+} = 14.76$ K	20 iterations

Table A16 (Channel 3, $\Delta T = \pm 1.0$ K)

T = 165 K	$\Delta T^{-} = -26.29$ K	19 iterations

BIBLIOGRAPHIC DATA SHEET

1 Report No.	2 Government Accession No.	3. Recipient's Catalog No.
TM 78058		

4. Title and Subtitle	5. Report Date
Calibration Analysis for a Multi-Channel Infrared Scanning Radiometer	December 1977
	6. Performing Organization Code 941
7. Author(s) Harvey Walden, Edward J. Hurley, and C. Laurence Korb	8. Performing Organization Report No.
9. Performing Organization Name and Address	10. Work Unit No.
NASA/Goddard Space Flight Center Greenbelt, Maryland	11. Contract or Grant No.
	13. Type of Report and Period Covered
12. Sponsoring Agency Name and Address	NASA Technical Memorandum
National Aeronautics and Space Administration Washington, D. C.	14 Sponsoring Agency Code

15. Supplementary Notes

16. Abstract

A procedure for calibrating an infrared scanning spectroradiometer by a computerized parametric error analysis technique is developed and described. The uncertainties in the radiometric measurements of scene radiance and (for the case of a blackbody scene) temperature due to possible uncertainties in the calibration target temperature, calibration target emissivity, and instrument temperature are calculated for a range of uncertainty levels in the parameters, as well as for a gamut of scene temperatures corresponding to a given spectral channel. This technique is applicable to the radiometric calibration of any infrared radiometer; in this paper, it has been applied specifically to the Cloud-Top Scanning (C.T.S.) Radiometer, a three-channel instrument designed for aircraft-borne cloud radiance measurements in the 6.75 and 11.5 μm thermal emission spectral regions.

17. Key Words (Selected by Author(s))	18. Distribution Statement
Infrared radiometer Radiometric calibration Radiance measurement	Unclassified—Unlimited

19 Security Classif. (of this report)	20 Security Classif (of this page)	21. No of Pages	22. Price*
Unclassified	Unclassified	68	

*For sale by the National Technical Information Service, Springfield, Virginia 22151